IQGAP1 promotes CXCR4 chemokine receptor function and trafficking via EEA-1+ endosomes

Adebowale O. Bamidele,[1,2] Kimberly N. Kremer,[2] Petra Hirsova,[3] Ian C. Clift,[2,4] Gregory J. Gores,[3] Daniel D. Billadeau,[2,5] and Karen E. Hedin[2]

[1]Department of Molecular Pharmacology and Experimental Therapeutics, [2]Department of Immunology, [3]Division of Gastroenterology and Hepatology, [4]Neurobiology of Disease Research Program, and [5]Division of Oncology Research, Mayo Clinic, Rochester, MN 55905

IQ motif–containing GTPase-activating protein 1 (IQGAP1) is a cytoskeleton-interacting scaffold protein. CXCR4 is a chemokine receptor that binds stromal cell–derived factor-1 (SDF-1; also known as CXCL12). Both IQGAP1 and CXCR4 are overexpressed in cancer cell types, yet it was unclear whether these molecules functionally interact. Here, we show that depleting IQGAP1 in Jurkat T leukemic cells reduced CXCR4 expression, disrupted trafficking of endocytosed CXCR4 via EEA-1+ endosomes, and decreased efficiency of CXCR4 recycling. SDF-1–induced cell migration and activation of extracellular signal-regulated kinases 1 and 2 (ERK) MAPK were strongly inhibited, even when forced overexpression restored CXCR4 levels. Similar results were seen in KMBC and HEK293 cells. Exploring the mechanism, we found that SDF-1 treatment induced IQGAP1 binding to α-tubulin and localization to CXCR4-containing endosomes and that CXCR4-containing EEA-1+ endosomes were abnormally located distal from the microtubule (MT)-organizing center (MTOC) in IQGAP1-deficient cells. Thus, IQGAP1 critically mediates CXCR4 cell surface expression and signaling, evidently by regulating EEA-1+ endosome interactions with MTs during CXCR4 trafficking and recycling. IQGAP1 may similarly promote CXCR4 functions in other cancer cell types.

Introduction

CXC chemokine receptor 4 (CXCR4) is a ubiquitously expressed G protein–coupled receptor (GPCR) that functions to promote cellular adhesion and chemotaxis and regulates gene expression through activation of extracellular signal-regulated kinases 1 and 2 (ERK) MAPK and other pathways (Busillo and Benovic, 2007). CXCR4 is frequently overexpressed in cancer and is a negative prognostic factor for epithelial-derived tumors, lymphomas, and leukemias (Teicher and Fricker, 2010). CXCR4 signals upon binding stromal cell–derived factor-1 (SDF-1; also called CXCL12), a chemokine expressed in bone marrow, lymph nodes, liver, lungs, and brain (Müller et al., 2001). SDF-1/CXCR4 signaling promotes cancer cell metastasis, retention, proliferation, and/or survival at sites of SDF-1 (Teicher and Fricker, 2010). IQ motif–containing GTPase-activating protein 1 (IQGAP1) is a multidomain scaffold protein that regulates the actin and microtubule (MT) networks, ERK, and gene expression in response to signaling by cell surface receptors (Roy et al., 2005; Neel et al., 2011; White et al., 2012; Liu et al., 2013; Carmon et al., 2014; Feigin et al., 2014). Like CXCR4, IQGAP1 is associated with cancer cell proliferation, metastasis, and invasion (Brown et al., 2007; White et al., 2009, 2011; Krishnan et al., 2012; Jameson et al., 2013). In immune cells, IQGAP1 is required to reorient the MT-organizing center

(MTOC) during natural killer cell–mediated cytotoxicity and for modulating T cell antigen receptor (TCR) signaling (Kanwar and Wilkins, 2011; Gorman et al., 2012). Although both IQGAP1 and CXCR4 have been associated with cancer and regulate the cytoskeleton, functional interactions between these proteins were previously unknown.

IQGAP1 associates with the cytoskeleton and binds several cytoskeletal regulatory proteins among many other proteins. IQGAP1 contains calponin homology (CH), IQ, WW, RasGAP-related domain (GRD), and RasGAP C-terminal (RGCT) domains that link IQGAP1 to F-actin, myosin, ERK, cytoskeletal-modulating GTPases Rac1 and CDC42, and the plus end MT–associated protein CLIP-170, respectively (White et al., 2012). CXCR4 binds SDF-1 at the cell surface and initiates signal transduction by activating heterotrimeric GTP-binding G proteins of the Gi, Gq, and G12/13 classes (Busillo and Benovic, 2007; Kumar et al., 2011). These G proteins signal to stimulate ERK and other kinases, activate integrins, and remodel the cytoskeleton to cause cellular chemotaxis. In addition, CXCR4 signaling stimulates its endocytosis, a process which reduces cell surface levels of CXCR4 and initiates CXCR4 intracellular trafficking. Receptor trafficking is often altered in cancer (Hoeller et al., 2006; Mosesson et al., 2008).

The Rockefeller University Press $30.00
J. Cell Biol. Vol. 210 No. 2   257–272
www.jcb.org/cgi/doi/10.1083/jcb.201411045

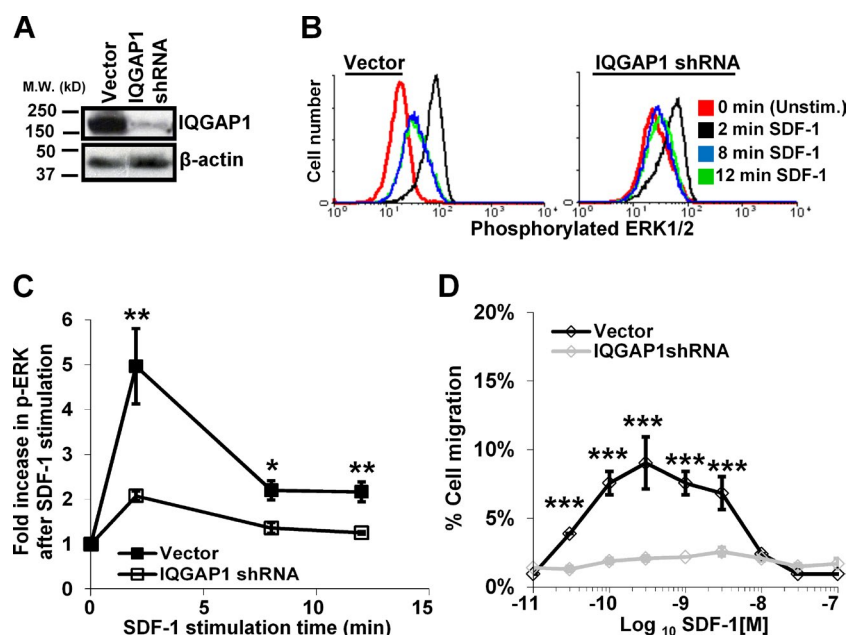JCB   257

THE JOURNAL OF CELL BIOLOGY

Figure 1. **Depletion of IQGAP1 via shRNA inhibits SDF-1–induced ERK activation and migration of Jurkat T leukemic cells.** Cells transfected with either IQGAP1 shRNA–encoding plasmid or vector control plasmid were analyzed 72 h later. Both plasmids also encoded GFP to enable identification of transfected cells. (A) Whole cell lysates were immunoblotted for IQGAP1; the same membrane was stripped and reblotted for β-actin as a control. (B) Cells were stimulated as indicated with SDF-1, and then active, phosphorylated ERK in GFP+ cells was determined via flow cytometric analysis of permeabilized cells incubated with specific mAb. Representative results are shown. (C) Summary of multiple experiments performed as in B and including B showing mean responses ± SEM; $n = 4$; *, $P < 0.05$; **, $P < 0.01$. (D) Cell migration was assayed in response to SDF-1 ± SD; $n = 4$; ***, $P < 0.001$. Result shown is representative of three independent experiments.

CXCR4 endocytosis occurs after receptor phosphorylation by GPCR kinases, which recruits β-arrestins to mediate CXCR4 endocytosis. CXCR4 traffics through early endosome antigen 1–containing (EEA-1+) endosomes and is then sorted either into recycling endosomes for return to the cell surface or lysosomes for degradation (Marchese and Benovic, 2001; Marchese et al., 2003; Neel et al., 2005; Bhandari et al., 2009; Malik et al., 2012; Marchese, 2014).

Here, we show that decreasing IQGAP1 expression in the Jurkat acute lymphoblastic leukemic T cell line significantly reduced cell surface expression of CXCR4 and impaired CXCR4 signaling in response to SDF-1, thereby limiting both chemotaxis and other downstream effects of this chemokine receptor. In contrast, the expression and constitutive trafficking of another receptor on these cells, the TCR, was unaffected by IQGAP1 depletion. We further show that these events arise from a previously unknown function of IQGAP1 as a critical regulator of CXCR4 trafficking at a step where CXCR4 cargo–containing EEA-1+ endosomes interact with the MT network. IQGAP1 similarly regulated CXCR4 trafficking and signaling in human epithelial and cholangiocarcinoma cell lines in addition to the leukemic cell line. Thus, IQGAP1 functionally modifies CXCR4 in several cancer cell types.

Results

Depletion of IQGAP1 protein via shRNA inhibits SDF-1–induced ERK activation and migration of Jurkat cells

Jurkat cells are derived from a human T cell acute lymphoblastic leukemia and expresses both IQGAP1 and CXCR4. We transfected Jurkat cells with a plasmid encoding both IQGAP1 shRNA and GFP. Control cells were transfected with the same plasmid vector encoding GFP alone. 72 h later, immunoblotting revealed a >96 ± 2.4% reduction of IQGAP1 protein in IQGAP1 shRNA–transfected cells as compared with control cells (Fig. 1 A). After treatment with SDF-1, active, phosphorylated ERK was assayed by flow cytometry after staining per-

meabilized cells with fluorescently conjugated phospho-ERK mAb. Electronic gating was used to assay ERK activation only in GFP+ (transfected) cells (Fig. 1 B). In multiple experiments, IQGAP1-depleted cells displayed significant defects in ERK activation (Fig. 1 C). In addition, Jurkat cells expressing only the control vector migrated toward SDF-1, but IQGAP1-deficient cells were defective (Fig. 1 D).

IQGAP1 depletion substantially reduces CXCR4 expression on the cell surface

To begin to address the mechanism, we first assayed the CXCR4 cell surface levels on intact cells. Jurkat cells transfected with the IQGAP1 shRNA plasmid progressively decreased their cell surface CXCR4 (Fig. 2 A). 72 h after transfection, CXCR4 cell surface levels were an average of 10 ± 1–fold lower on IQGAP1-depleted cells as compared with control cells (Fig. 2 B). Second, we measured total cellular CXCR4 protein via CXCR4 mAb staining of fixed and permeabilized cells, showing this was reduced by ∼40% (Fig. 2 C). Third, we measured CXCR4 mRNA via real-time quantitative RT-PCR in IQGAP1-depleted cells and found that this was reduced by ∼60% (Fig. 2 D). As controls, we showed that CXCR4 shRNA similarly reduced CXCR4 protein expression (Fig. 2 C) and that IQGAP1 depletion had no significant effect on the cell surface levels of another receptor, the TCR (Fig. 2 E). A second IQGAP1 shRNA similarly reduced CXCR4 cell surface expression and inhibited SDF-1–induced ERK activation (Fig. S1). Other shRNAs expressed from the same plasmid vector but directed against other proteins do not affect either CXCR4 cell surface levels or signaling in Jurkat (Kremer et al., 2011a,b). Together, these results indicate that IQGAP1 regulates the expression of CXCR4.

Defective SDF-1–induced ERK activation and migration in IQGAP1-deficient cells are not restored by rescuing CXCR4 expression

To address whether the signaling defects in Fig. 1 simply reflect decreased cell surface CXCR4, CXCR4 expression was
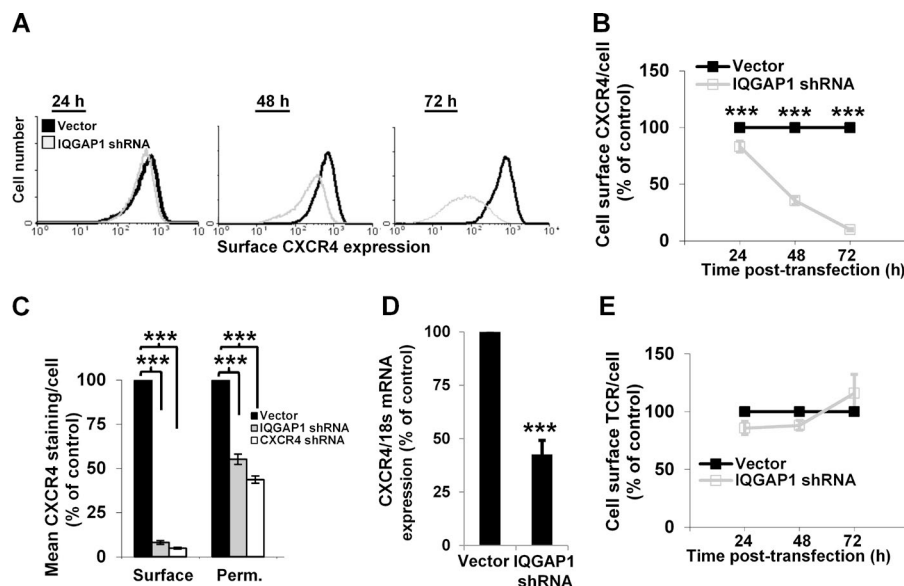
A

24 h   48 h   72 h

Cell number

■ Vector
□ IQGAP1 shRNA

Surface CXCR4 expression

B

Cell surface CXCR4/cell (% of control)

■ Vector
□ IQGAP1 shRNA

***   ***   ***

Time post-transfection (h)

C

Mean CXCR4 staining/cell (% of control)

*** *** *** ***

■ Vector
▨ IQGAP1 shRNA
□ CXCR4 shRNA

Surface   Perm.

D

CXCR4/18s mRNA expression (% of control)

***

Vector   IQGAP1 shRNA

E

Cell surface TCR/cell (% of control)

■ Vector
□ IQGAP1 shRNA

Time post-transfection (h)

Figure 2. **IQGAP1 depletion substantially reduces CXCR4 expression on the cell surface.** Jurkat cells were transfected as in Fig. 1. (A) Cell surface CXCR4 levels determined by FACS of transfected (GFP⁺) cells decreased with time after transfection. Representative results are shown. (B) Summary of multiple experiments as in A ± SEM; $n = 4$. (C) Mean cell surface (Surface) and total cellular (Perm.) CXCR4 protein per cell was determined via flow cytometry 72 h after transfection ± SEM; $n = 3$. Positive control, Jurkat transfected with CXCR4 shRNA. (D) CXCR4 mRNA determined via quantitative RT-PCR 72 h after transfection. Bars denote mean results compared with 18s mRNA ± SEM; $n = 3$. (E) No significant differences were seen in TCR cell surface expression in the same cells from A and B; means ± SEM are shown; $n = 4$. For B–D: ***, $P < 0.001$.

restored in IQGAP1-deficient Jurkat cells by cotransfecting a plasmid encoding YFP-tagged CXCR4 (CXCR4-YFP). This strategy increased cell surface CXCR4 on IQGAP1-deficient cells, yielding near-normal (+) or approximately twice-normal (++) cell surface CXCR4, without altering either TCR cell surface levels (Fig. 3 A) or the extent of IQGAP1 protein depletion (Fig. 3 B). Nevertheless, IQGAP1-deficient cells expressing CXCR4-YFP remained unable to efficiently activate ERK in response to SDF-1 (Fig. 3 C). Similarly, restoring CXCR4 expression failed to rescue defective SDF-1–dependent migration of IQGAP1-deficient cells (Fig. 3, D and E). Similar results were seen when CXCR4 expression was rescued by forced expression of wild-type CXCR4 instead of CXCR4-YFP (Fig. S2, A–C). SDF-1/CXCR4-induced ERK activation and cell migration require pertussis toxin (PTX)–sensitive Gi proteins (Dutt et al., 1998; Kumar et al., 2006). To address whether IQGAP1 deficiency affects Gi protein coupling to CXCR4, we more directly assayed Gi protein activation by measuring inhibition of cAMP after forskolin activation of adenylyl cyclase (Dessauer et al., 1997). As expected, in vector-transfected cells, SDF-1 inhibited forskolin-induced cAMP production in a PTX-sensitive manner (Fig. 3 F, black bars; Cheng et al., 2000). Interestingly, depleting IQGAP1, as in Fig. 3 (A–C), had no detectable effect on the ability of SDF-1 to inhibit forskolin-induced cAMP levels (Fig. 3 F, white and gray bars). Thus, IQGAP1 is not required for Gi protein coupling to CXCR4 but is required for ERK activation and cell migration.

IQGAP1 colocalizes with endocytosed CXCR4 after SDF-1 treatment

We asked whether IQGAP1 might participate in regulating CXCR4 trafficking. Jurkat cells were transfected with a plasmid encoding fluorescently tagged CXCR4 (CXCR4-YFP), an approach we previously used to study CXCR4 trafficking (Kumar et al., 2006, 2011). Consistent with previous studies (Fukata et al., 2002; Kumar et al., 2006, 2011; Fernández-Arenas et al., 2014), CXCR4-YFP localized primarily to the plasma membranes of unstimulated cells, whereas IQGAP1 was located just under the plasma membrane, consistent with a location within the cortical cytoskeleton (Fig. 4 A). In response to SDF-1, CXCR4-YFP underwent endocytosis and trafficked into clustered

endosomes, and IQGAP1 was detected colocalizing with endocytosed CXCR4 (Fig. 4, A and B). Quantitation confirmed that endocytosed CXCR4 colocalized with IQGAP1 in ~60% of cells after 30 min of SDF-1 treatment (Fig. 4 C).

IQGAP1 depletion disrupts the intracellular trafficking of endocytosed CXCR4 into endosomes clustered near the MTOC

We next asked whether IQGAP1 deficiency alters CXCR4 endocytosis and/or intracellular trafficking. Endocytosis of both endogenous CXCR4 and CXCR4-YFP in response to SDF-1 was readily detected in IQGAP1-deficient cells (Fig. 5 A). Quantitation revealed that, although it was less efficient, CXCR4 and CXCR4-YFP endocytosis occurred in IQGAP1-deficient cells (Fig. 5 B). We then assayed postendocytic trafficking of CXCR4-YFP ± SDF-1 stimulation of live, IQGAP1-deficient cells. In both control and IQGAP1 shRNA–expressing unstimulated cells, CXCR4-YFP was mainly expressed on the cell surface (Fig. 5 C, 0-min images). As described previously (Kumar et al., 2011), applying SDF-1 to control cells for 15–30 min provoked CXCR4-YFP endocytosis and trafficking into a centrally clustered endosomal compartment (Fig. 5 C, top). In contrast, the postendocytic trafficking of CXCR4-YFP was abnormal in IQGAP1-deficient cells, with endocytosed CXCR4-YFP residing in scattered, rather than clustered, endosomes (Fig. 5 C, bottom). Quantitation confirmed that IQGAP1 shRNA–expressing cells displayed defective localization of endocytosed CXCR4-YFP into clustered endosomes after either 15 or 30 min of SDF-1 treatment (Fig. 5 D). Finally, we performed the same experiment as in Fig. 5 C, except that the MTOC was visualized by fixing and staining for α-tubulin. Consistent with a previous study (Kumar et al., 2011), SDF-1 treatment of control cells evoked CXCR4-YFP endocytosis and trafficking into endosomes clustered near the MTOC (Fig. 5 E, left). In contrast, the endocytosed CXCR4-YFP of IQGAP1-deficient cells trafficked into endosomes that lacked association with the MTOC (Fig. 5 E, right). Quantitation revealed that after 5–30 min of SDF-1, an increasing proportion of vector transfected cells, but not IQGAP1 shRNA–transfected cells, displayed at least 30% of their CXCR4-YFP⁺ endosomes clustered near the MTOC (Fig. 5, F and G). Yet even after 30 min of SDF-1 treatment, few
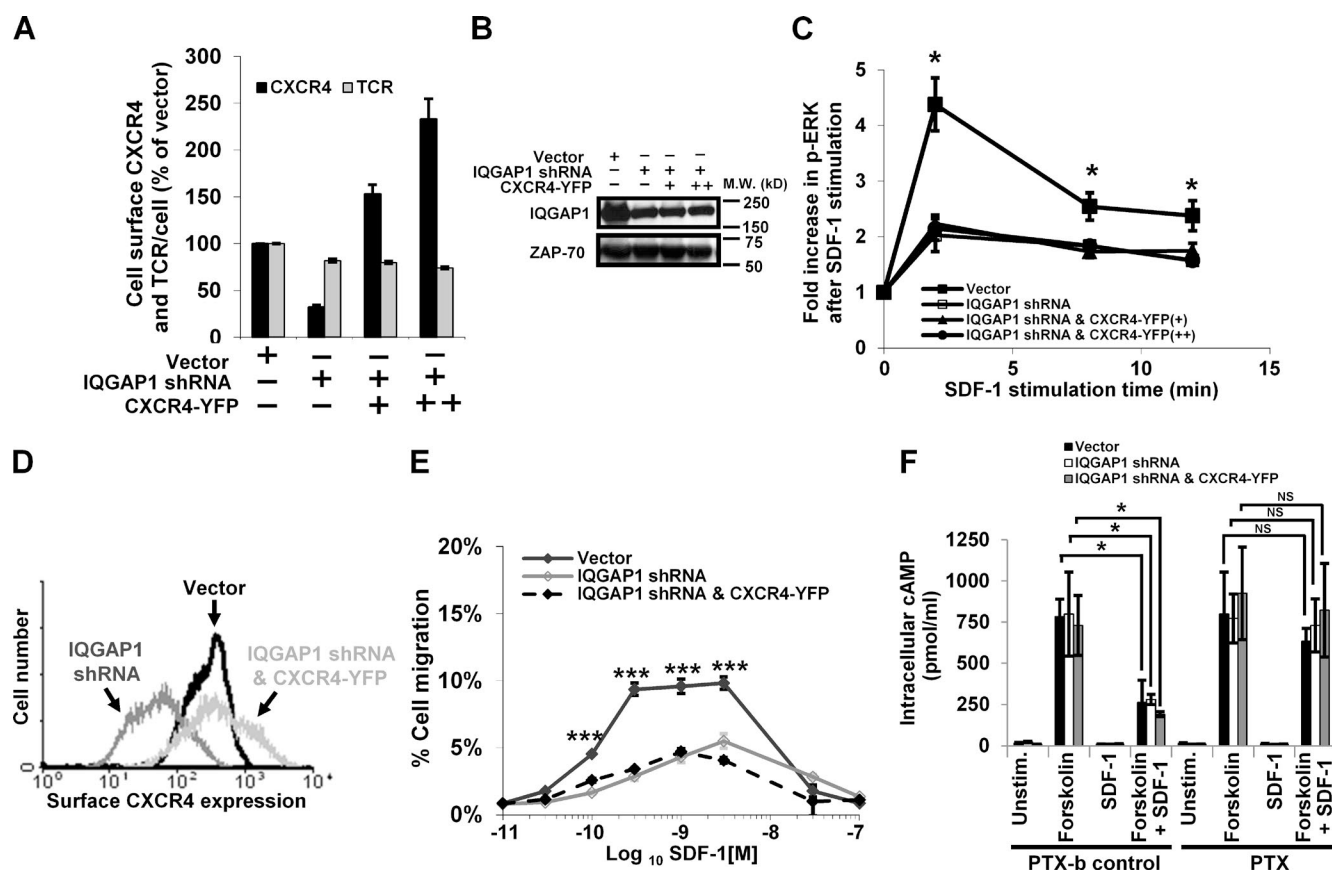
Figure 3. **Defective SDF-1–induced ERK activation and migration in IQGAP1-deficient cells are not restored by rescuing CXCR4 expression.** (A–C) Jurkat cells were transfected as in Figs. 1 and 2 plus either no (−), low (+), or high (++) amounts of CXCR4-YFP. (A) 48 h after transfection, CXCR4 and TCR cell surface levels were determined as in Fig. 2 (B and E). Bars denote means ± SEM; $n = 3$. (B) Whole cell lysates of cells from experiments in A and C, immunoblotted with IQGAP1 and ZAP-70 as a control. (C) ERK activation was assayed as in Fig. 1 (B and C). Mean results of multiple experiments are shown ± SEM; $n = 4$; *, $P < 0.05$. (D and E) Cells transfected as in A–C were analyzed 72 h later for CXCR4 cell surface expression as in Fig. 2 A (D) or migration as in Fig. 1 D (E). Mean migration ± SD is shown; $n = 4$; ***, $P < 0.001$. (F) Cells transfected as in A–C were pretreated with either PTX-b (control) or PTX and then assayed for SDF-1–mediated inhibition of forskolin-induced cAMP. Bars denote the mean cAMP ± SD; $n = 3$; *, $P < 0.05$. For A, E, and F, each is representative of three independent experiments.

IQGAP1 shRNA–expressing cells showed even 30% of their CXCR4-YFP[+] endosomes clustered near the MTOC (Fig. 5, F and G). Collectively, these results indicate that IQGAP1 depletion markedly inhibits the postendocytic trafficking of CXCR4 into endosomes clustered near the MTOC.

IQGAP1-deficient cells display abnormal CXCR4 trafficking via EEA-1^{+} endosomes

CXCR4 traffics through EEA-1^{+} endosomes in response to SDF-1 treatment of HEK293 epithelial cells (Marchese et al., 2003; Bhandari et al., 2007; Malik and Marchese, 2010). We assayed this trafficking step in IQGAP1-deficient cells via mAb staining of fixed cells. After 5-min SDF-1 treatment of control cells, 94 ± 2.6% of endocytosed CXCR4-YFP was colocalized with EEA-1 (Fig. 6, A [left] and B [black bars]). By 30 min, endocytosed CXCR4-YFP in control cells was beginning to traffic beyond early endosomes, as reflected by the reduced colocalization of CXCR4-YFP and EEA1^{+} at 30 versus 5 min (Fig. 6, A [left] and B [black bars]). In contrast, IQGAP1 shRNA–expressing cells displayed significantly delayed colocalization of endocytosed CXCR4-YFP with EEA-1: only 21 ± 9.0% of cells displayed CXCR4-YFP colocalization with EEA-1 after 5 min of SDF-1 treatment, and this increased to 82 ± 7.3% at 30 min (Fig. 6, A [right] and B [gray bars]). Consistent with these re-

sults, IQGAP1 deficiency impaired the ability of endocytosed CXCR4 to traffic into downstream Rab7^{+} endosomes (Fig. 6, C [top row] and D). IQGAP1 deficiency was also associated with abnormal subcellular localization of the lysosomal-associated membrane protein 2[+] (LAMP2^{+}) lysosomal compartment at the periphery of the cell and with a significant fraction of the endocytosed CXCR4 entering these lysosomes (Fig. 6, C [bottom row] and E). Thus, IQGAP1 deficiency causes abnormal intracellular trafficking of endocytosed CXCR4, which is evident at the EEA-1^{+} and also potentially other endosomal stages.

IQGAP1 regulates EEA-1^{+} endosome location relative to the MT cytoskeleton and increases α-tubulin binding in response to SDF-1

Molecular motors mediate the progressive trafficking of protein cargo through endosomes associated with MTs (Lansbergen et al., 2004; Provance et al., 2004); thus, we investigated the locations of EEA-1^{+} endosomes relative to the MTOC. In addition to IQGAP1 shRNA, cells expressed YFP-tagged tubulin to visualize the MTOC and were stained with EEA-1. Both control vector– and IQGAP1 shRNA–transfected cells displayed an MT network that reoriented slightly relative to the fibronectin-coated coverslip in response to treatment with SDF-1; no
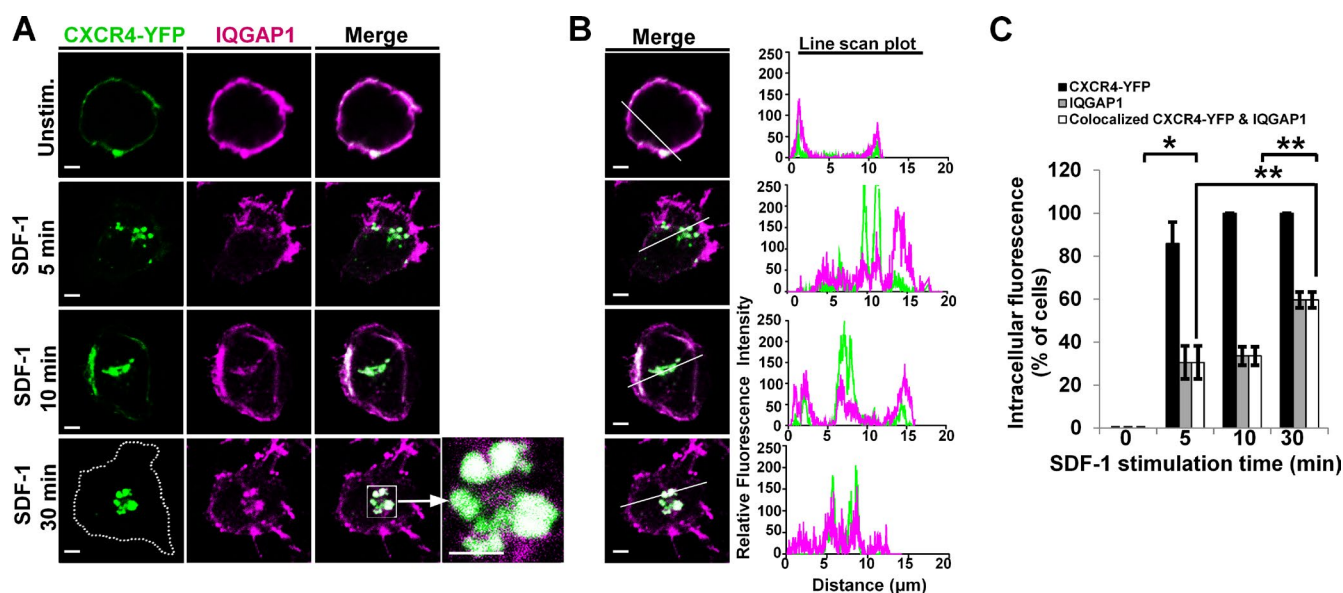
Figure 4. IQGAP1 colocalizes with endocytosed CXCR4 after SDF-1 treatment. Jurkat cells were transfected with CXCR4-YFP, stimulated with SDF-1, and then fixed and stained for YFP and IQGAP1. (A) Representative cell images of 15–30 cells imaged per condition analyzed on three separate days. The dotted line denotes the plasma membrane as seen on DIC images; the boxed region is expanded to show IQGAP1 and CXCR4-YFP colocalization. (B) Line scan intensity profiles of merged images in A. (C) Quantitation of multiple experiments performed as in A and B and including A and B, showing the change in the percentage of cells displaying intracellular CXCR4-YFP, IQGAP1, or colocalized CXCR4-YFP and IQGAP1 at the indicated times after SDF-1 addition ± SEM; $n = 3$; *, $P < 0.05$; **, $P < 0.01$; bars, 2 µm.

abnormalities in the organization of either the MT cytoskeleton or the MTOC were apparent in IQGAP1-deficient cells (Fig. 7 A). In contrast, EEA-1⁺ endosomes in IQGAP1-deficient cells were abnormal in their locations relative to the MTOC both before and after SDF-1 stimulation (Fig. 7 A) and were distributed relatively evenly along MTs instead of being located nearer to the MTOC (Fig. 7 A). Quantitation revealed a relative deficiency of EEA-1⁺ endosomes clustering near the MTOC in IQGAP1-deficient cells (Fig. 7 B). Moreover, SDF-1 treatment of control cells but not IQGAP1-deficient cells enhanced the clustering of EEA-1⁺ endosomes near the MTOC (Fig. 7 B), consistent with EEA-1⁺ endosomes moving toward the MTOC in response to cytoskeletal reorganization stimulated by SDF-1/CXCR4 signaling. IQGAP1 depletion via shRNA had no effect on either EEA-1 or α-tubulin protein expression (Fig. 7 C). IQGAP1 binds α-tubulin (Fukata et al., 2002); therefore, we asked whether this association was enhanced after SDF-1–induced CXCR4 endocytosis and trafficking. Jurkat cells were stimulated with SDF-1, and α-tubulin was immunoprecipitated and analyzed for binding to IQGAP1. SDF-1 treatment for 5–15 min transiently increased the interaction of IQGAP1 with α-tubulin, subsiding to basal levels after 30 min (Fig. 7 D). Together, the results in Fig. 7 indicate that IQGAP1 transiently increases its interactions with MTs in response to SDF-1 and that this occurs during the time when IQGAP1 is required to permit CXCR4-containing EEA-1⁺ endosomes to associate with MTs in a manner that facilitates SDF-1–induced CXCR4 trafficking into endosomal compartments near the MTOC.

IQGAP1 is similarly required for CXCR4 signaling and trafficking via EEA-1⁺ endosomes in KMBC cholangiocarcinoma and HEK293 cell lines

The role of IQGAP1 in cholangiocarcinoma is unknown, but CXCR4 plays a role in progression (Gentilini et al., 2012; Rizvi and Gores, 2013). Similar to Jurkat, IQGAP1 depletion in KMBC and HEK293 cells impaired CXCR4 trafficking through EEA-1⁺ endosomes, and the EEA-1⁺ endosomes were abnormally located relative to the MTOC (Fig. 8, A–D). Also similar to Jurkat, both KMBC and HEK293 originally expressed endogenous cell surface CXCR4 (Fig. 8 E) and displayed reduced CXCR4 mRNA levels after IQGAP1 depletion (Fig. 8 G). Forced overexpression of CXCR4 successfully equalized CXCR4 cell surface levels on vector- and IQGAP1 shRNA–transfected cells (Fig. 8 H); nevertheless, IQGAP1 depletion significantly inhibited CXCR4 signaling (Fig. 8 I).

IQGAP1 depletion in Jurkat cells similarly impairs the trafficking and signaling of an ectopically expressed GPCR, DOR1

The δ-opioid receptor (DOR1), like CXCR4, is coupled to Gi proteins, activates ERK, and is endocytosed and undergoes intracellular trafficking in response to ligand (Kramer et al., 2000; Zhang et al., 2005; Gendron et al., 2015). DOR1 endocytosis and signaling occurs in T cells, but roles for EEA-1 endosomes and IQGAP1 were unknown (Heagy et al., 1990; Hedin et al., 1999; Law et al., 2000). Jurkat does not express endogenous DOR1. We used a Jurkat subline stably expressing FLAG-tagged DOR1 (Hedin et al., 1997). Depletion of IQGAP1 did not detectably alter cell surface DOR1 on unstimulated cells (Fig. 9, A and B). Deltorphin (agonist)-induced DOR1 endocytosis was slightly impaired (Fig. 9 B); however, DOR1 intracellular trafficking was abnormal in IQGAP1-deficient cells: endocytosed DOR1 was delayed in colocalizing with EEA-1⁺ endosomes (Fig. 9, C, E, and F) and failed to traffic into endosomes clustered near the MTOC (Fig. 9, D, E, and G). Moreover, DOR1 signaling leading to ERK activation was significantly defective in IQGAP1-deficient cells (Fig. 9 H). Thus, in addition to CXCR4, other GPCRs may also be critically regulated by IQGAP1.
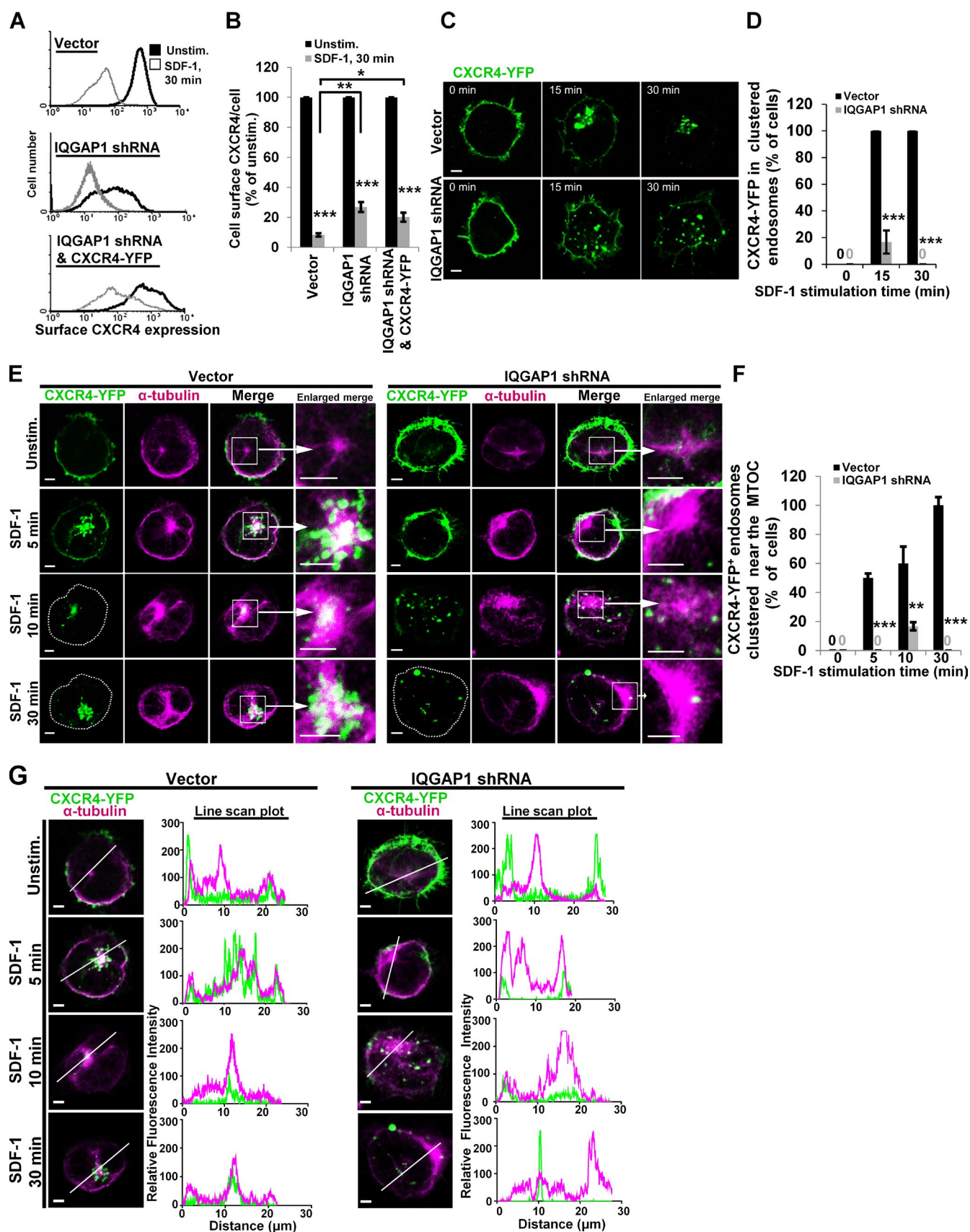
Figure 5. **IQGAP1 depletion disrupts the intracellular trafficking of endocytosed CXCR4 into endosomes clustered near the MTOC.** Jurkat cells were transfected as in Fig. 3, and then CXCR4 endocytosis and trafficking were analyzed as indicated. (A and B) CXCR4 endocytosis in response to 30-min SDF-1 treatment was assayed by FACS. (A) Representative result of three separate experiments. (B) Summary of all three experiments performed as in A

IQGAP1 is required for efficient CXCR4 recycling after SDF-1 stimulation

A substantial proportion of CXCR4 endocytosed in response to SDF-1 traffics into recycling endosomes and subsequently recycles back to the cell surface (Malik and Marchese, 2010; Kumar et al., 2011). Recycling endosomes are typically located proximal to the MTOC (Kumar et al., 2011). We showed above (Figs. 5 and 8) that CXCR4 intracellular trafficking near the MTOC was disrupted in IQGAP1-deficient cells; therefore, we asked whether CXCR4 recycling was also inhibited. Jurkat cells expressing either IQGAP1 shRNA or a control plasmid were pretreated with either the protein synthesis inhibitor cycloheximide (CHX) or vehicle (DMSO) and then treated with SDF-1 to induce CXCR4 endocytosis. SDF-1 was subsequently washed away, and the cells were incubated for an additional 1 h to permit receptor recycling back to the cell surface. This process was monitored by assaying cell surface CXCR4 levels at different times. In control cells, $30 \pm 5.0\%$ of the endogenous CXCR4 originally located on the cell surface recycled back to the cell surface (Fig. 10 A, Vector DMSO bars). A similar fraction of CXCR4 recycled when CHX was included in the experiment, confirming that receptor recycling is being measured rather than de novo protein synthesis (Fig. 10 A, Vector CHX bars). As discussed above (Figs. 2, 5, and 6), IQGAP1 shRNA–transfected cells display abnormally low levels of CXCR4 on the cell surface. Nevertheless, the CXCR4 on IQGAP1-deficient cells responded to SDF-1 by undergoing endocytosis (Fig. 10 A, IQGAP1 shRNA bars). Unlike in control cells, no significant recycling of endocytosed CXCR4 was detected in IQGAP1-deficient cells (Fig. 10 A, IQGAP1 shRNA bars). The same data in Fig. 10 A are replotted in Fig. 10 B after normalization to the levels of cell surface CXCR4 after SDF-1 treatment. Fig. 10 C is a control showing that CHX effectively inhibited protein synthesis in these experiments because it reduced the abundance of short half-life protein Mcl-1 (Derouet et al., 2004). These results suggested that, in the absence of IQGAP1, CXCR4 might be inhibited in its ability to traffic into recycling endosomes. We previously showed that CXCR4 traffics into Rab11+ recycling endosomes in Jurkat cells stimulated with SDF-1 (Kumar et al., 2011). Interestingly, this trafficking step was significantly defective in IQGAP1-depleted cells (Fig. 10 D). Quantitation of multiple experiments performed as in Fig. 10 D revealed that in vector control cells, $67 \pm 7.4\%$ of CXCR4-YFP+ endosomes colocalized with Rab11+ endosomes after 30 min of SDF-1 treatment compared with only $2.8 \pm 1.7\%$ in IQGAP1-depleted cells.

Model for IQGAP1 regulation of CXCR4 trafficking and signaling in leukemic cells

Based on our results, we propose the model of IQGAP1 modification of CXCR4 functions shown in Fig. 10 E. After SDF-1 treatment, IQGAP1 promotes CXCR4 endocytosis and more critically mediates the postendocytic trafficking of CXCR4 via EEA-1+ endosomes. IQGAP1 is required to enhance EEA-1+ endosomal clustering near the MTOC, perhaps via a process in which IQGAP1 transiently binds to the plus ends of MTs to permit endosomal movement toward the MTOC. For this reason, CXCR4 in IQGAP1-deficient cells displays defective trafficking and reduced recycling via Rab11+ endosomes to the plasma membrane. Because of its critical role in promoting CXCR4 trafficking, IQGAP1 is required for SDF-1/CXCR4-dependent signal transduction that relies on CXCR4 endocytosis and trafficking, including activation of ERK and directional cell migration.

Discussion

CXCR4 promotes cancer cell metastasis, proliferation, and survival (Teicher and Fricker, 2010). Leukemic and several other types of cancer stem cells use CXCR4 to metastasize and persist in bone marrow niches rich in SDF-1 that support their homing, survival, and resistance to chemotherapy (Burger and Kipps, 2006; Zeng et al., 2009). Cancer progression is fostered by expression and overexpression of CXCR4, which causes increased CXCR4 signaling in niches where SDF-1 is highly expressed (Shen et al., 2001; Konoplev et al., 2007; Gentilini et al., 2012; Rizvi and Gores, 2013). Here, we describe a novel role for the IQGAP1 scaffold protein as a critical regulator of CXCR4 receptor trafficking and cell surface expression and show that IQGAP1 functions to regulate CXCR4 trafficking through EEA-1+ endosomes.

We found that SDF-1 stimulation provoked IQGAP1 to move from its basal location just under the plasma membrane to colocalize with endosomes containing endocytosed CXCR4. Depletion of IQGAP1 impaired the trafficking of endocytosed CXCR4 via EEA-1+ endosomes, which inhibited subsequent CXCR4 trafficking, including CXCR4 recycling to the cell surface via Rab11+ endosomes. Instead, the aberrantly trafficked CXCR4 in IQGAP1-deficient cells appeared to enter LAMP2+ lysosomes. Protein cargo in other cell types progressively traffics through endosomes via association with MTs (Lansbergen et al., 2004; Provance et al., 2004), and CXCR4 traffics and recycles in leukemic cells via Rab11+ recycling endosomes clustered near the MTOC (Kumar et al., 2011). Interestingly, SDF-1 treatment increased IQGAP1's association with α-tubulin at the time when IQGAP1 colocalized with endocytosed CXCR4; we also found that IQGAP1 depletion resulted in the abnormal subcellular location of CXCR4-containing EEA-1+ endosomes distal from the MTOC. Together, our results support a model in which IQGAP1 functions to promote CXCR4 trafficking

and including A, showing substantial, but nevertheless deficient, SDF-1–induced endocytosis in IQGAP1-deficient cells. Means ± SEM; $n = 3$. (C and D) CXCR4-YFP intracellular trafficking visualized via confocal imaging of live, transfected cells 48 h after transfection. 0-min confocal images were taken, then SDF-1 was added, and additional images of the same cell were taken 15 and 30 min later. (C) Representative z-slice images of 11–13 cells analyzed on three separate days. (D) Results of multiple experiments performed as in C and including C, showing the percentage of cells analyzed in each day's experiment in which CXCR4-YFP–containing endosomes were clustered ± SEM; $n = 3$ experiments. (E–G) Jurkat cells transfected as in C and D were analyzed 72 h later. Cells were stimulated ± SDF-1 and then fixed and stained as in Fig. 4 A for YFP and α-tubulin. (E) Representative images of 15–30 cells analyzed per condition from experiments performed on three separate days. The dotted lines denote the plasma membrane as seen in DIC images. The area within each cell with the highest α-tubulin staining (the MTOC) was enlarged to show the clustering of CXCR4-YFP–containing endosomes in control (Vector) but not IQGAP1 shRNA–transfected cells. (F) Quantitation of multiple experiments as in E, showing the mean percentage of cells analyzed in each day's experiment in which ≥30% of the CXCR4-YFP–containing endosomes in the cell were clustered near the MTOC ± SEM; $n = 3$. (G) Line scan intensity profiles in merged images from E. For B–F: *, $P < 0.05$; **, $P < 0.01$; ***, $P < 0.001$; bars, 2 µm.
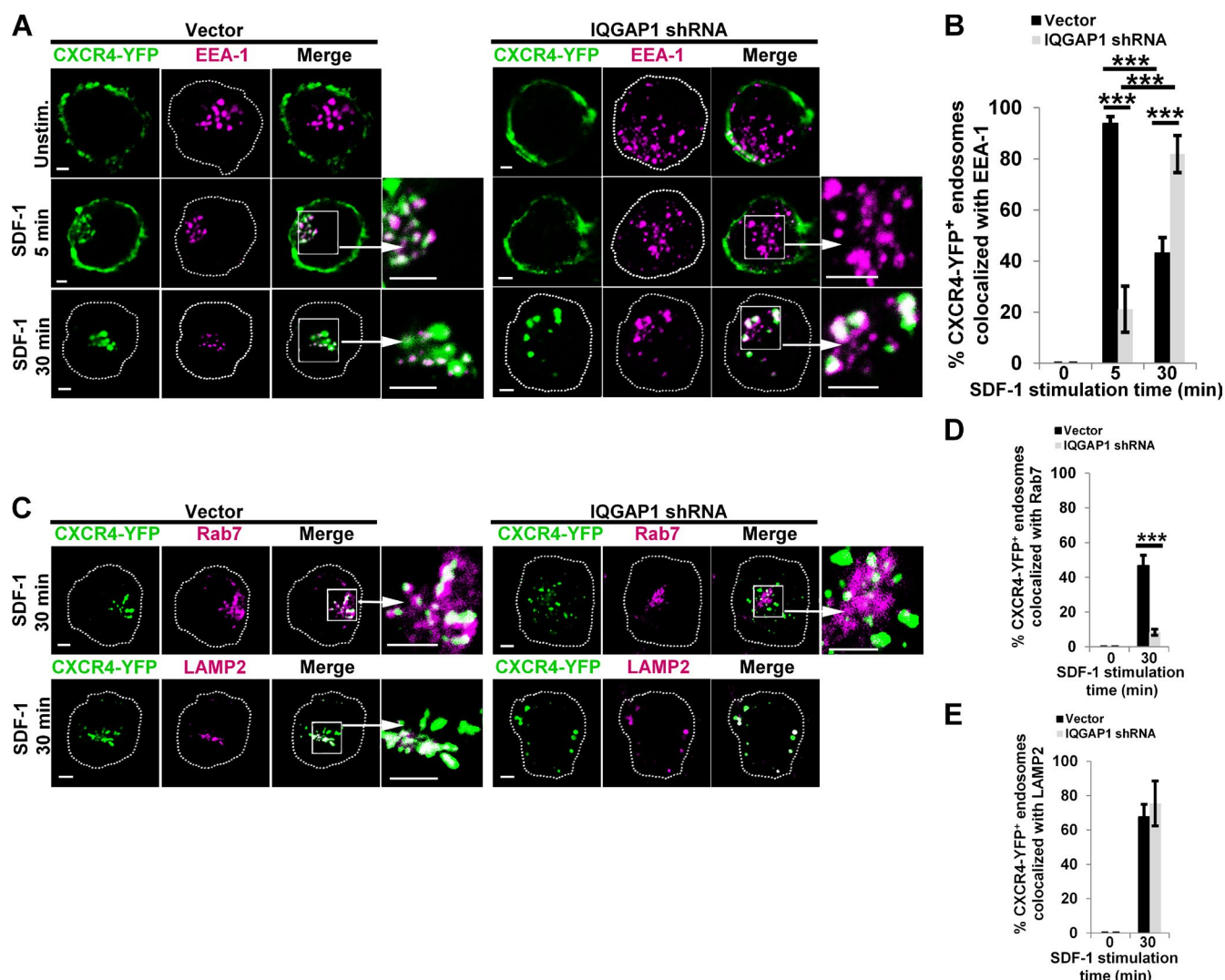
Figure 6. IQGAP1-deficient Jurkat cells display abnormal CXCR4 trafficking via EEA-1+ endosomes. Jurkat cells were transfected as in Fig. 5 (E and F). 48 h later, cells were stimulated with SDF-1 and then fixed and stained for YFP, EEA-1, Rab7, and/or LAMP2. (A) Representative images are shown; the boxed EEA-1+ regions are enlarged; dotted lines denote the plasma membrane as seen on DIC images. (B) Quantitation of multiple experiments as in A, showing the mean percentage of CXCR4-YFP+ endosomes colocalizing with EEA-1+ vesicles in each cell analyzed in each day's experiment ± SEM. (C) Representative images are shown. Box, enlarged to show colocalization of CXCR4-YFP and IQGAP1. (D and E) Quantitation of multiple experiments as in C, showing the mean percentage of CXCR4-YFP+ endosomes that colocalized with Rab7+ or LAMP2+ vesicles in each cell analyzed in each day's experiment ± SEM. For A–E: n = 3 experiments; ***, P < 0.001; bars, 2 µm.

through EEA-1+ endosomes by helping to link these endosomes to MTs and thereby promote CXCR4 trafficking through EEA-1+ endosomes into recycling endosomes clustered near the MTOC (Fig. 10 D). These results are likely to be broadly applicable to understanding CXCR4 expression and function in leukemic and other cell types. In addition to Jurkat, we noted similar effects of IQGAP1 on CXCR4 trafficking and signaling in KMBC cholangiocarcinoma and HEK293 cell lines.

This is the first study to indicate that IQGAP1 regulates the trafficking and recycling of a chemokine receptor via the EEA-1+ endosomal compartment. IQGAP1 could function in this role by physically linking EEA-1+ endosomes to the plus ends of MTs, perhaps via binding to CLIP-170, an MT plus end–binding protein that has been shown to bind to IQGAP1 and that mediates cargo trafficking by linking cargo-containing endosomes to MTs (Pierre et al., 1992; Lansbergen et al., 2004; Nakano et al., 2010). IQGAP1 may facilitate the movement of

CXCR4-containing EEA-1+ endosomes along MTs toward the MTOC with the help of molecular motors (Lansbergen et al., 2004; Provance et al., 2004). Because we found that IQGAP1's association with endocytosed CXCR4 occurred in response to SDF-1, the regulation of CXCR4 trafficking through the EEA-1+ endosomal compartment by IQGAP1 may arise from ligand-initiated signaling by this GPCR. IQGAP1 may similarly participate in mediating EEA-1+ endosome regulation by other GPCRs, as we showed here that IQGAP1 deficiency impairs the intracellular trafficking and signaling of DOR1 expressed in Jurkat cells. Other types of receptors evidently traffic via IQGAP1-independent mechanisms. For example, we found no evidence that IQGAP1 regulates the trafficking of another receptor on these cells, the TCR, consistent with studies indicating that the TCR traffics via a distinctive mechanism (Fig. S3; Finetti et al., 2009, 2014). Interestingly, the EGF receptor utilizes G proteins to promote EEA-1+ endosome maturation
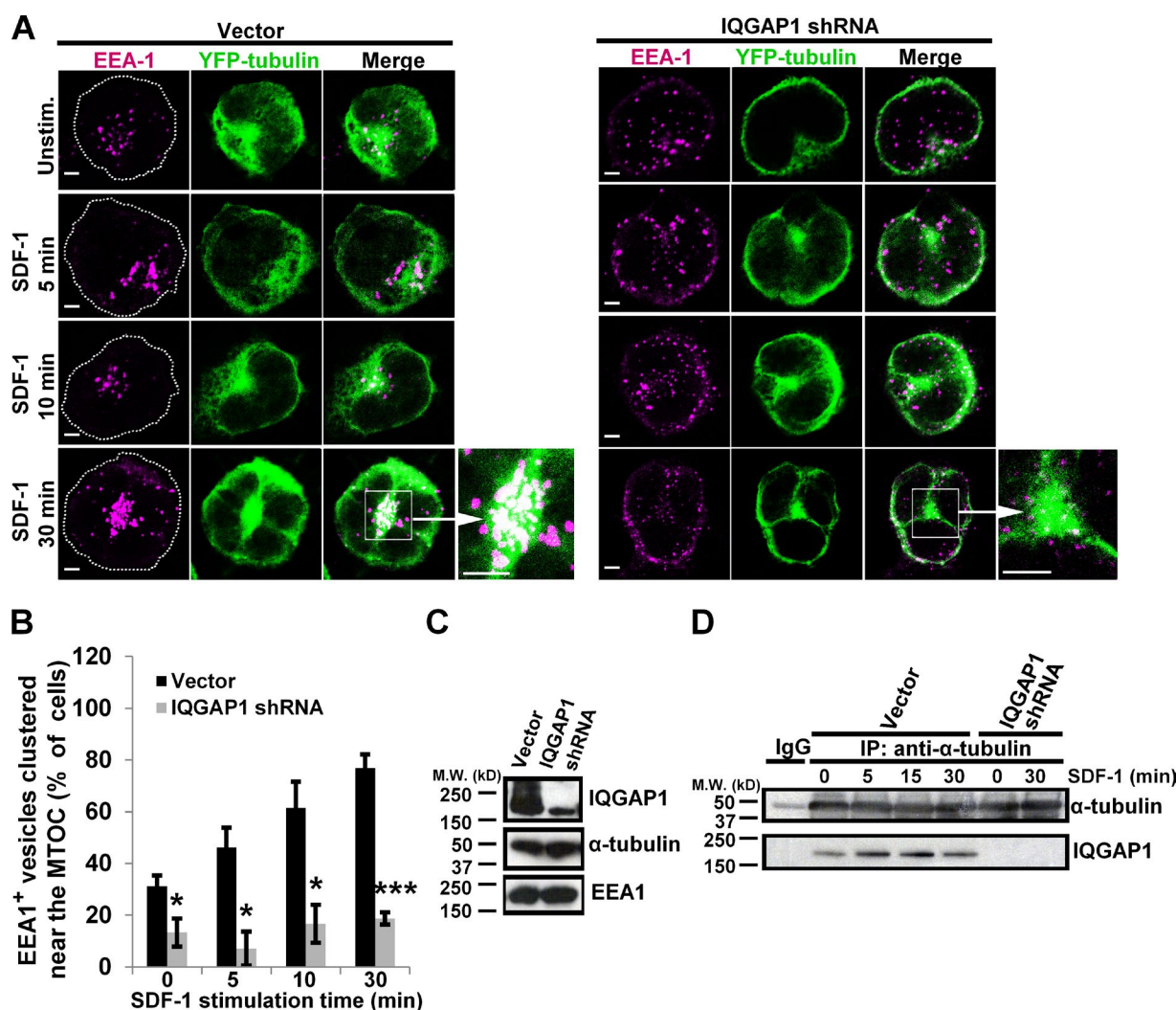
Figure 7. **IQGAP1 regulates EEA-1⁺ endosome location relative to the MT cytoskeleton.** Jurkat cells were transfected as in Fig. 5 (E and F) plus YFP-tagged tubulin. 72 h later, cells were stimulated with SDF-1 and then fixed and stained for EEA-1 and YFP. (A) Representative results; dotted lines denote the plasma membrane as seen on DIC images; the boxed MTOC areas are enlarged. Bars, 2 μm. (B) Quantitation of multiple experiments as in A, showing the percentage of cells in which $\geq$30% of EEA-1⁺ endosomes clustered near the MTOC ± SEM; n = 3; *, P < 0.05; ***, P < 0.001. (C) Immunoblot of whole cell lysates from A and B. (D) Jurkat cells were transfected with vector or IQGAP1 shRNA as in Fig. 1. 72 h later, cells were stimulated with SDF-1, lysed, immunoprecipitated with either anti–α-tubulin or control IgG, and immunoblotted with IQGAP1 and α-tubulin. Result is representative of three independent experiments.

in epithelial cells (Beas et al., 2012). Other receptors may also use IQGAP1 for trafficking. Indeed, CXCR2 has been shown to bind IQGAP1 in neutrophils (Neel et al., 2005, 2011), and the TGF-β II receptor utilizes IQGAP1 for lysosomal trafficking in hepatic stellate cells (Liu et al., 2013).

We also show here that IQGAP1 depletion inhibits downstream outcomes of SDF-1/CXCR4 signaling, including activation of ERK and cellular chemotaxis in response to SDF-1, while having no detectable effect on Gi protein coupling to CXCR4. Even under conditions of forced CXCR4 overexpression, we found that IQGAP1-deficient cells displayed defective ERK and migration responses to SDF-1. IQGAP1 could promote CXCR4-induced ERK activation by acting as a scaffold for ERK pathway proteins (Mataraza et al., 2003). Alternatively or in addition, the ability of IQGAP1 to promote CXCR4 receptor endocytosis, intracellular trafficking, and recycling is expected to enhance the downstream effects of SDF-1. In T lymphocytes, CXCR4 endocytosis has been shown to promote coupling to

ERK signaling (Cheng et al., 2000). CXCR4 endocytosis brings activated receptors near the RasGRP1 and N-Ras molecules located on the Golgi complex that are required for SDF-1–induced ERK activation in these cells (Bivona et al., 2003; Caloca et al., 2003; Zugaza et al., 2004; Kremer et al., 2011b). Moreover, endocytosed CXCR4 forms heterodimers with the TCR within Rab11⁺ endosomes, and these CXCR4-TCR heterodimers critically enhance ERK activation in response to SDF-1 (Kumar et al., 2006, 2011). Alternatively, CXCR4 might be signaling to activate ERK from endosomal compartments after its endocytosis and trafficking, as has been seen for other GPCRs (Shenoy and Lefkowitz, 2005). Cellular chemotaxis in response to chemokines also relies on receptor endocytosis, which is required for the polarized recycling of receptors to the leading edge and for directional cell migration (Nieto et al., 1997; Masztalerz et al., 2007; Kumar et al., 2011; Morgan et al., 2013).

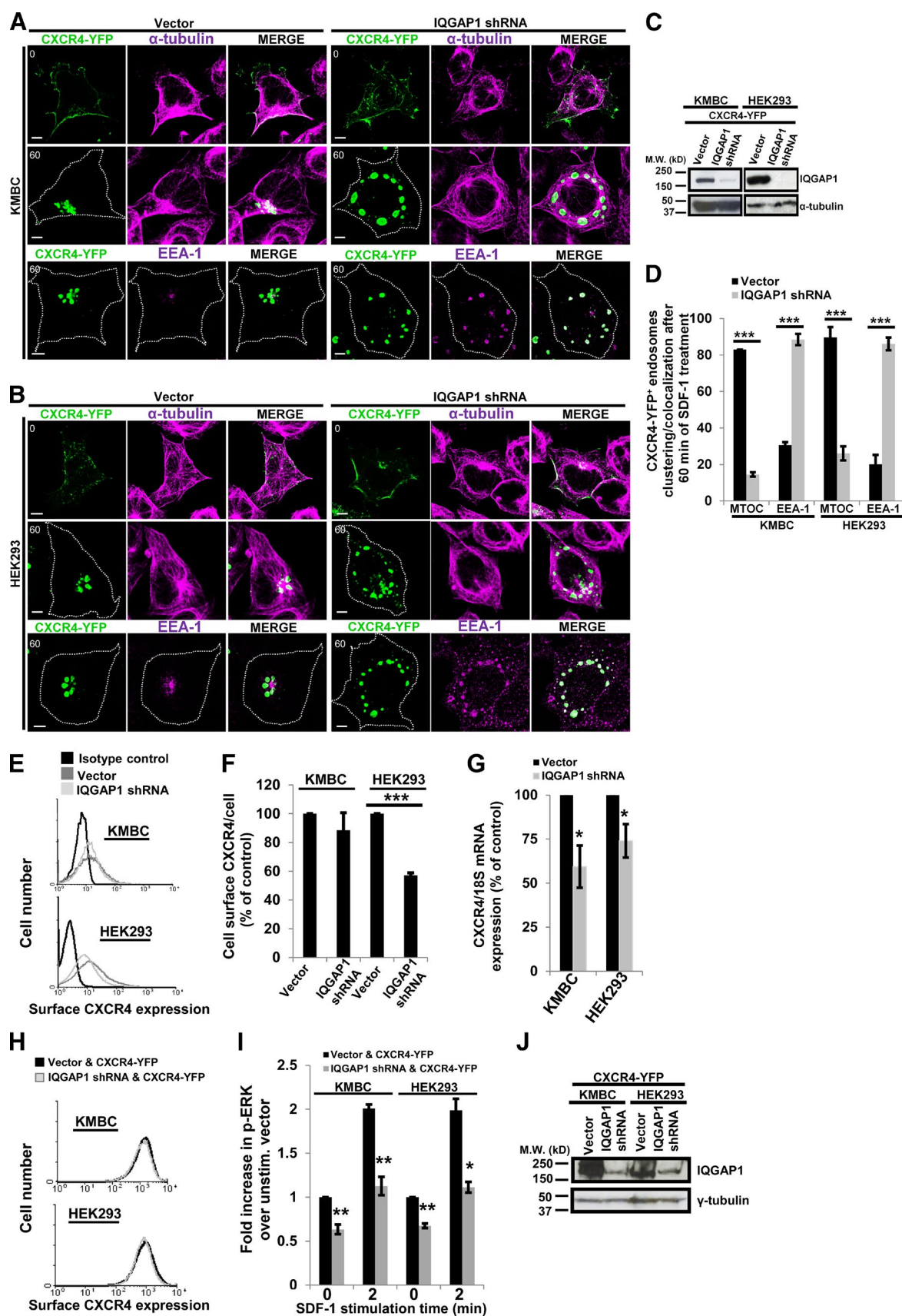The functional interactions described here between IQGAP1 and CXCR4 are likely to have significant clinical

Figure 8. **IQGAP1 is similarly required for CXCR4 signaling and trafficking via EEA-1⁺ endosomes in KMBC cholangiocarcinoma and HEK293 cell lines.** (A and B) The indicated cell lines were transfected and analyzed as in Figs. 5 E and 6 A. The dotted lines denote the plasma membrane as seen on DIC images. Representative images are shown after 0 or 60 min of SDF-1 treatment. Bars, 5 µm. (C) Whole cell lysates of cells in A and B were immunoblotted

implications. There is emerging clinical interest in inhibiting IQGAP1 functions in cancer therapy (Jameson et al., 2013; Stuart and Sellers, 2013). Our results indicate that these approaches are likely to be even more effective because of synergistic inhibitory effects of IQGAP1 depletion on CXCR4 trafficking, cell surface expression, and function. Interestingly, in addition to the effects on CXCR4 trafficking, reducing IQGAP1 protein levels significantly decreased CXCR4 mRNA expression in three different cell types. Although the mechanism responsible is not known, IQGAP1 may regulate the CXCR4 promoter because IQGAP1 deficiency had no effect on CXCR4 expression levels derived from a plasmid (Fig. S2 D), and IQGAP1 has been shown to be capable of indirectly regulating gene transcription via several mechanisms (Malarkannan et al., 2012; Goto et al., 2013; Erdemir et al., 2014). Together, the results presented here indicate that IQGAP1 is a potent regulator of CXCR4 expression, trafficking, and function, including in cancer cells.

Materials and methods

Cells, stimulation conditions, and statistical analysis

The Jurkat T cell line and Jurkat cells stably expressing murine DOR1 tagged with Flag (Jurkat-DOR1-FLAG cells; Sharp et al., 1996) were maintained in medium A (RPMI 1640 supplemented with 10% FCS, 10 mM Hepes, pH 7.4, and 2 mM L-glutamine) at <10^6 cells/ml. In brief, the coding sequence of DOR1 (Bzdega et al., 1993) that is N-terminally Flag tagged (Flag-DOR1) was obtained from M. Von Zastrow (University of California, San Francisco, San Francisco, CA; Tsao and von Zastrow, 2000). Flag-DOR1 was then cloned into HindIII–XhoI sites in the REP-9 expression vector (Invitrogen) and then transfected into Jurkat cells, and G418-resistant, FLAG-positive cells were sorted using anti-Flag mAb M2. Human cholangiocarcinoma KMBC and human embryonic kidney (HEK) 293 cell lines were maintained in DMEM 10% FCS, 4.5 g/liter D-glucose, L-glutamine, and 100 mg/liter sodium pyruvate. Unless otherwise noted, cell stimulations were performed at 37°C with either 50 nM SDF-1α (R&D Systems) or 5 × 10^{-6} M Deltorphin (RBI). Where indicated, cells were also treated with 100 ng/ml PTX, 100 ng/ml PTX-b oligomer, and/or 0.25 mM forskolin (EMD Millipore). Statistical analysis was via two-tailed t test (Microsoft Excel software) and the means of two distributions were considered significantly different if P < 0.05, P < 0.01, or P < 0.001.

Transient transfection, plasmids, immunoblotting, and immunoprecipitation

All transient transfections were performed by electroporating 10^7 cells at 315 V for 10 ms (Jurkat) or 240 V for 15 ms (other cells), as described previously (Kumar et al., 2006). Cells were analyzed 48–72 h later; transfection efficiencies were 70–80%. shRNAs were expressed under control of the H1 promoter from either pCMS3-cherry-H1P or pCMS4-eGFP-H1P, plasmid vectors which also each encode a fluorescent protein driven by the SV40 promoter to mark individual cells expressing shRNA (Gomez et al., 2006; Kumar et al., 2006; Gorman et al., 2012). The IQGAP1 shRNA was 5′-GTCCT-

GAACATAATCTCAC-3′ in either pCMS3-cherry-H1P or pCMS4-eGFP-H1P and was previously used in Gorman et al. (2012). A second IQGAP1 shRNA (5′-GGGTGTTGCTGAGAAGACT-3′) was cloned into pCMS4-eGFP-H1P and used for Fig. S1. The CXCR4 shRNA was 5′-CAGGAGTGGGGTTGATTTCA-3′ cloned into pCMS4-eG-FP-H1P. The plasmid encoding C-terminally tagged YFP fluorescent fusion proteins of human CXCR4 (CXCR4-YFP) and human CD3-ζ cDNAs (CD3-ζ–YFP) driven by the CMV promoter were made by separately subcloning CXCR4 and CD3-ζ cDNAs into p-EYFP-N1vector (Takara Bio Inc.) as previously described (Kumar et al., 2006); the plasmid encoding YFP (p-EYFP) tagged to the N terminus of human α-tubulin (YFP-tubulin) driven by the CMV promoter was from Takara Bio Inc. Untagged human CXCR4 cDNA was cloned into pCMS4-m.Cherry-HIP and used for Fig. S2. For immunoblotting, the indicated cells were lysed with Mg^{2+} Lysis/Wash Buffer (EMD Millipore). Whole cell lysates were analyzed by SDS-PAGE and immunoblotting for IQGAP1 using mouse monoclonal anti-IQGAP1 (EMD Millipore). As controls, the same membranes were stripped and reprobed with either mouse monoclonal anti–β-actin (Novus Biologicals) or rabbit polyclonal anti–ZAP-70 (Santa Cruz Biotechnology, Inc.). IQGAP1 knockdown efficiency was quantitated using ImageJ (National Institutes of Health). Background-subtracted experimental band densities were normalized to densities of β-actin control bands in the same lanes. For immunoprecipitation, the indicated cell lysates were incubated with protein G–agarose beads (Sigma-Aldrich) plus either mouse IgG control or mouse monoclonal α-tubulin mAb (Sigma-Aldrich) overnight at 4°C. The beads were precipitated, washed, and then analyzed by SDS-PAGE. Membranes were immunoblotted with anti-IQGAP1, and then the same membranes were stripped and reprobed with anti–α-tubulin as a control.

Assays of active, phosphorylated ERK1 and ERK2

Cells were transfected by electroporation with the indicated plasmids and cultured for 72 h. Cells were then stimulated, fixed with Lyse/Fix Buffer (BD) for 10 min at 37°C, and then washed with Stain Buffer (FBS; BD) and permeabilized with Perm Buffer III (BD) for 30 min at 4°C. Excess Perm Buffer III was washed off three times with Stain Buffer, and active ERK of transfected (GFP+) cells was determined by flow cytometry after staining with anti-ERK1/2(pT202/pY204) conjugated to Alexa Fluor 647 (BD) as described previously (Kremer et al., 2011a).

Chemotaxis assays

Jurkat cells were transfected as indicated with either IQGAP1 shRNA and GFP or empty vector– and GFP-expressing plasmids. 72 h later, chemotaxis assays were performed using 96-well Chemotx chemotaxis plates (Neuroprobe) with 5 μm-pore filters coated with fibronectin (Invitrogen). Cells (500,000) were diluted in Migration Buffer (RPMI without phenol red supplemented with 0.5% BSA and 1% DMSO) and placed in the upper chamber of each well. After migrating at 37°C for 1 h toward lower chambers containing the indicated concentrations of SDF-1, cells remaining in the upper chambers were removed, and cells that migrated into the lower chambers were quantified by measuring GFP (485 nm ex/530 nm em) fluorescence using a Cytofluor 4000 spectrometer (PerSeptive Biosystems).

---

for IQGAP1 or α-tubulin as a control. (D) Multiple experiments as in A and B were quantitated as in Figs. 5 F and 6 B ± SEM. (E and F) Cell surface CXCR4 levels of cells in A–D were assayed in Fig. 2 A. (E) Representative results. (F) Means of multiple experiments as in E ± SEM. (G) CXCR4 mRNA levels of cells in A–D were assayed as in Fig. 2 D ± SEM. (H) CXCR4-YFP expression in cells as in A–D performed as in Fig. 3; representative result is shown. (I) Cells expressing CXCR4-YFP as in H were stimulated with SDF-1 and assayed for active ERK as in Fig. 3 C; bars show means ± SEM. (J) Whole cell lysates of cells in H and I were immunoblotted for IQGAP1 and γ-tubulin as a control. For D, F, G, and I: $n = 3$; *, P < 0.05; **, P < 0.01; ***, P < 0.001.
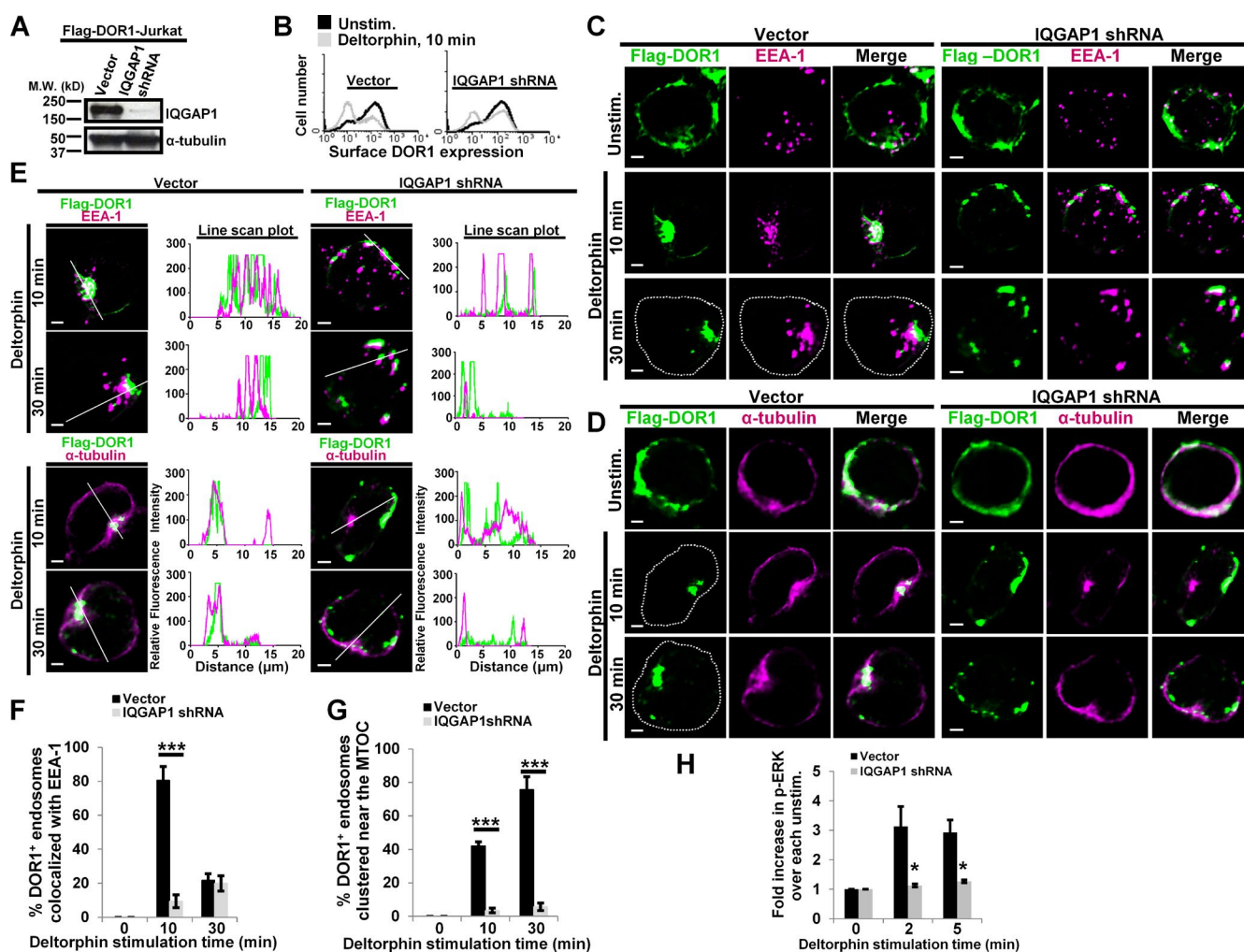
Figure 9. **IQGAP1 depletion in Jurkat cells similarly impairs the trafficking and signaling of an ectopically expressed GPCR, DOR1.** (A) Jurkat cells stably expressing FLAG-tagged DOR1 were transfected either with IQGAP1 shRNA or a control plasmid as in Fig. 1 A. 72 h later, whole cell lysates were immunoblotted to confirm depletion of IQGAP1 protein. (B) Flow cytometric assay of cell surface DOR1 ± treatment with the DOR1 agonist, Deltorphin; $n = 3$. (C–E) Deltorphin-induced DOR1 trafficking was assayed as in Fig. 6 A, except that DOR1 was visualized with anti-FLAG. (C and D) Representative images of 15–30 cells analyzed per condition on three separate days are shown. Dotted lines denote the plasma membrane as seen on DIC images. (E) Line scan intensity profiles of the indicated selected merged images from C and D; bars, 2 μm. (F and G) Quantitation as in Figs. 5 F and 6 B of multiple experiments performed as in C and D ± SEM. (H) DOR1-expressing Jurkat cells depleted of IQGAP1 as in A–G were stimulated with Deltorphin and assayed for ERK activation as in Fig. 1 C. Bars denote means ± SEM. For F–H: $n = 3$; *, $P < 0.05$; ***, $P < 0.001$.

Intracellular cAMP assay

Jurkat cells were transfected with vector-m.Cherry or IQGAP shR-NA-m.Cherry plasmids ± a plasmid encoding a YFP-tagged CXCR4 (CXCR4-YFP). 48 h after transfection, 10^6 cells/ml were pretreated with either PTX or control toxin (PTX-b) at 100 ng/ml for 4 h and then stimulated with SDF-1 or SDF-1 plus 0.25 mM forskolin for 5 min. Reactions were stopped by lysing cells in 0.1 M HCl. cAMP was measured using a cAMP EIA kit (Cayman Chemical Company) according to the manufacturer's instructions with a Synergy H1-Multi Mode Absorbance plate reader (BioTek).

Assays of cell surface CXCR4 and TCR, assay of CXCR4 endocytosis and recycling, and assay of total cellular CXCR4

Jurkat cells were transfected as indicated with either IQGAP1 shRNA and GFP or empty vector– and GFP-expressing plasmids. 24–72 h later, either CXCR4 or TCR-CD3ε mAb conjugated to allophycocyanin (APC; R&D Systems) was used to stain intact cells. The cell surface levels of each receptor were quantitated via flow cytometry of transfected (GFP⁺) cells. To assay CXCR4 recycling, we used the method described previ-

ously (Grundler et al., 2009; Kumar et al., 2011), which allows sufficient time for recycling but not for de novo CXCR4 protein synthesis. In brief, cells were treated either with vehicle (DMSO) or 10 μg/ml CHX (Sigma-Aldrich) for 2 h before and during the experiment. Cells were then treated with SDF-1 for 30 min, washed three times with PBS, and either stained immediately for CXCR4 or incubated for 1 h in culture media, and then CXCR4 cell surface levels were assayed via flow cytometry. To assay total cellular CXCR4, cells were fixed and permeabilized as for ERK assays (Kremer et al., 2011a) and then stained with CXCR4-APC mAb, and then GFP⁺ cells were analyzed by flow cytometry.

Assays of DOR1 cell surface levels

Jurkat-DOR1-FLAG stable cells were transfected with plasmids expressing either IQGAP1 shRNA and m.Cherry or empty vector and m.Cherry. 72 h later, cells were stimulated with Deltorphin or vehicle control as indicated, and cell surface DOR1 protein expression on m.Cherry⁺ cells was assayed by flow cytometry after staining intact cells with 10^{-7} M DOR1 antagonist, naloxone conjugated to FITC (Molecular Probes), at room temperature for 10 min (Hedin et al., 1997).
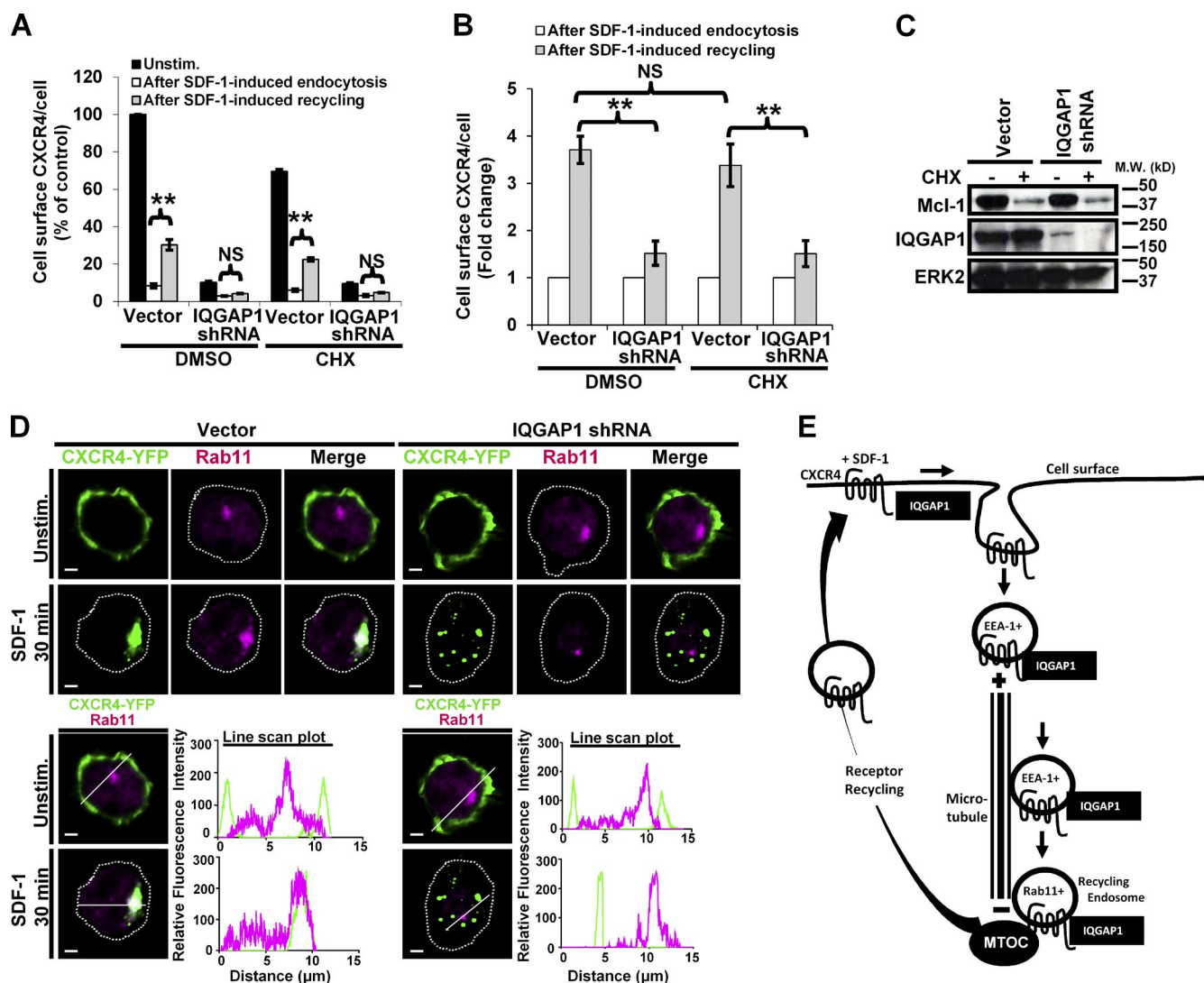
Figure 10. **IQGAP1 is required for efficient CXCR4 recycling after SDF-1 stimulation.** (A–C) Jurkat cells were transfected as in Fig. 1 and then assayed for the ability of CXCR4 to recycle back to the cell surface after endocytosis as follows. Either CHX or vehicle (DMSO) was applied to cells before and during the experiment to prevent de novo protein synthesis. CXCR4 cell surface levels were determined by FACS as in Fig. 2 A. (A) Results for unstimulated cells (black bars), cells immediately after 30 min of SDF-1 treatment (white bars), and cells after 30 min of SDF-1 treatment, washing, and additional incubation at 37°C for 1 h to allow CXCR4 recycling (gray bars). Means are shown normalized to CXCR4 levels on control cells (DMSO-treated, vector-transfected, unstimulated cells) ± SEM; $n = 4$; **, $P < 0.01$. (B) Same results as in A, replotted to show the fold changes. (C) Control immunoblot showing IQGAP1 protein depletion. Mcl-1 blot confirms CHX inhibition of protein synthesis; total ERK2 is a loading control. (D) Jurkat cells were transfected as in Fig. 5 E, treated with SDF-1, and then fixed and stained for YFP and Rab11. Representative images (top) and line scan intensity profiles of the indicated selected merged images (bottom) of 15–30 cells analyzed per condition on three separate days are shown; dotted lines denote the plasma membrane as seen on DIC images; bars, 2 µm. (E) See Model for IQGAP1 regulation of CXCR4 trafficking and signaling in leukemic cells in Results.

Quantitative PCR

Total RNA from transfected cells was isolated with the RNeasy Plus Mini kit (QIAGEN) and reverse transcribed with an iScript cDNA Synthesis kit (Bio-Rad Laboratories). Quantification of gene expression was performed by quantitative real-time RT-PCR using SYBR green fluorescence on a LightCycler 480 instrument (Roche). Primers used were CXCR4 forward, 5′-GGCCCTCAAGACCACAGTCA-3′; CXCR4 reverse, 5′-TTAGCTGGAGTGAAAACTTGAAG-3′; 18S forward, 5′-CGCTTCCTTACCTGGTTGAT-3′; and 18S reverse, 5′-GAGCGACCAAAGGAACCATA-3′. Target gene expression was calculated using the ΔΔCt method. Expression was normalized to 18S expression levels, which were stable across the experimental conditions. Data shown represent fold change as compared with vector-transfected cells analyzed in the same experiment.

Immunofluorescence assay of fixed cells

Cells were transiently transfected with the indicated constructs, including pCMS3-cherry-H1P (vector control) or IQGAP1 shRNA in pCMS3-cherry-H1P. 48–72 h later, cells were plated on 4-well Lab-Tek chamber slides (Thermo Fisher Scientific) coated with fibronectin for 4 h. Cells were treated with either SDF-1 or Deltorphin for the indicated times at 37°C, then fixed with 3% paraformaldehyde for 10 min, permeabilized with 0.15% Triton X-100 Surfact-Amps Detergent (Thermo Fisher Scientific) for 5 min, blocked for 30 min at room temperature with PBS containing 5% BSA and 0.1% glycine, and incubated with either primary antibody or conjugated primary antibody at 4°C overnight. Primary antibodies used were mouse monoclonal anti–EEA-1 (1:500; BD), rabbit polyclonal anti-GFP–Alexa Fluor 488 (1:1,000; Invitrogen), mouse monoclonal anti–α-tubulin and –γ-tubulin

(1:500; Sigma-Aldrich), rabbit polyclonal anti-Rab11 (1:200; Abcam), rabbit monoclonal anti-Rab7 (1:100; Cell Signaling Technology), mouse monoclonal anti-LAMP2 (0.5 µg/ml; Abcam), rabbit monoclonal anti-FLAG (5 µg/ml; Sigma-Aldrich), or mouse monoclonal anti-IQGAP1 (2 µg/ml; EMD Millipore) antibodies. After washing with PBS, slides were incubated with a secondary detection reagent (goat anti–mouse IgG– or goat anti–rabbit IgG–Alexa Fluor 647, 1:1,000; Invitrogen) for 1 h at room temperature, washed, and mounted using Prolong Antifade with DAP1 (Invitrogen). Images of transfected (m.Cherry$^+$ and or YFP$^+$) cells were captured by using C-Apochromat 63× objective/1.20 W korr M27 of a fluorescent confocal microscope (LSM 780 AxioObserver; Carl Zeiss). Images were processed using the Zen lite 2012 software (Carl Zeiss). Images of transfected cells were analyzed as follows. To quantitate the percentage of cells that displayed CXCR4-YFP colocalization with IQGAP1, 15–30 cells from three separate experiments performed on different days were analyzed. To quantitate DOR1 or CXCR4-YFP colocalization with EEA-1, 15–30 cells from three separate experiments performed on different days were analyzed, and the number of endosomal vesicles in each cell positive for CXCR4-YFP or DOR1 was compared with the number of endosomal vesicles in that cell positive for both CXCR4-YFP or DOR1 and EEA-1. To quantitate clustering of CXCR4-YFP or DOR1-containing endosomes near the MTOC, 15–30 cells from three separate experiments performed on different days were analyzed; the MTOC was defined as area of the highest intensity of α-tubulin fluorescence in each cell, and the number was scored of cells that displayed ≥30% CXCR4-YFP$^+$ or DOR1$^+$ endosomes clustered within a 1/5-cell-diameter circle centered on the MTOC. Line scan plots were performed by drawing a line across an area of interest and generating and plotting fluorescence values using Prism (GraphPad Software) and ImageJ/Fiji.

Confocal imaging of live cells expressing CXCR4-YFP fluorescent fusion protein

Cells were transfected with a plasmid encoding CXCR4-YFP, plus either pCMS3-cherry-H1P (vector control) or IQGAP1 shRNA in pCMS3-cherry-H1P. 48 h later, SDF-1–induced CXCR4-YFP trafficking was assayed in live cells before and after SDF-1, as previously described (Kumar et al., 2011). In brief, 48 h after transient transfection, cells were resuspended in an imaging medium (RMP1 supplemented with 10% FCS, 10 mM Hepes, pH 7.4, and 2 mM L-glutamine) and then plated on fibronectin-coated Delta T dishes 0.17 mm (Bioptechs Inc.) for 4 h. Cells were imaged before and after 15–30 min of SDF-1 treatment using a 37°C stage on an LSM 5 Live laser-scanning confocal microscope with I00× oil immersion objective (Carl Zeiss). Images were processed using the Zen lite 2012 software. Transfected (m.Cherry$^+$ and CXCR4-YFP$^+$) cell images were analyzed for CXCR4-YFP distribution from the plasma membrane to endosomal compartments after SDF-1 treatment.

Online supplemental material

Fig. S1 shows the effect of transiently expressing IQGAP1 shRNA #2 on reducing IQGAP1 protein expression, endogenous CXCR4 cell surface expression, and SDF-1–induced p-ERK1/2 in Jurkat cells. Fig. S2 shows that coexpressing untagged CXCR4 with IQGAP1 shRNA rescued CXCR4 cell surface expression but failed to rescue SDF-1–induced ERK activation in IQGAP1-depleted Jurkat cells. Fig. S3 shows that IQGAP1 depletion had no effect on the constitutive trafficking of TCR/CD3-ζ–YFP to the MTOC, evident by CD3-ζ–YFP colocalization with the MTOC in the absence of IQGAP1 characterized by disorganized EEA-1$^+$ vesicles. Online supplemental material is available at http://www.jcb.org/cgi/content/full/jcb.201411045/DC1. Additional data are available in the JCB DataViewer at http://dx.doi.org/10.1083/jcb.201411045.dv.

References

Beas, A.O., V. Taupin, C. Teodorof, L.T. Nguyen, M. Garcia-Marcos, and M.G. Farquhar. 2012. Gαs promotes EEA1 endosome maturation and shuts down proliferative signaling through interaction with GIV (Girdin). *Mol. Biol. Cell.* 23:4623–4634. http://dx.doi.org/10.1091/mbc.E12-02-0133

Bhandari, D., J. Trejo, J.L. Benovic, and A. Marchese. 2007. Arrestin-2 interacts with the ubiquitin-protein isopeptide ligase atrophin-interacting protein 4 and mediates endosomal sorting of the chemokine receptor CXCR4. *J. Biol. Chem.* 282:36971–36979. http://dx.doi.org/10.1074/jbc.M705085200

Bhandari, D., S.L. Robia, and A. Marchese. 2009. The E3 ubiquitin ligase atrophin interacting protein 4 binds directly to the chemokine receptor CXCR4 via a novel WW domain-mediated interaction. *Mol. Biol. Cell.* 20:1324–1339. http://dx.doi.org/10.1091/mbc.E08-03-0308

Bivona, T.G., I. Pérez De Castro, I.M. Ahearn, T.M. Grana, V.K. Chiu, P.J. Lockyer, P.J. Cullen, A. Pellicer, A.D. Cox, and M.R. Philips. 2003. Phospholipase Cγ activates Ras on the Golgi apparatus by means of RasGRP1. *Nature.* 424:694–698. http://dx.doi.org/10.1038/nature01806

Brown, M.D., L. Bry, Z. Li, and D.B. Sacks. 2007. IQGAP1 regulates *Salmonella* invasion through interactions with actin, Rac1, and Cdc42. *J. Biol. Chem.* 282:30265–30272. http://dx.doi.org/10.1074/jbc.M702537200

Burger, J.A., and T.J. Kipps. 2006. CXCR4: a key receptor in the crosstalk between tumor cells and their microenvironment. *Blood.* 107:1761–1767. http://dx.doi.org/10.1182/blood-2005-08-3182

Busillo, J.M., and J.L. Benovic. 2007. Regulation of CXCR4 signaling. *Biochim. Biophys. Acta.* 1768:952–963. http://dx.doi.org/10.1016/j.bbamem.2006.11.002

Bzdega, T., H. Chin, H. Kim, H.H. Jung, C.A. Kozak, and W.A. Klee. 1993. Regional expression and chromosomal localization of the delta opiate receptor gene. *Proc. Natl. Acad. Sci. USA.* 90:9305–9309. http://dx.doi.org/10.1073/pnas.90.20.9305

Caloca, M.J., J.L. Zugaza, and X.R. Bustelo. 2003. Exchange factors of the RasGRP family mediate Ras activation in the Golgi. *J. Biol. Chem.* 278:33465–33473. http://dx.doi.org/10.1074/jbc.M302807200

Carmon, K.S., X. Gong, J. Yi, A. Thomas, and Q. Liu. 2014. RSPO-LGR4 functions via IQGAP1 to potentiate Wnt signaling. *Proc. Natl. Acad. Sci. USA.* 111:E1221–E1229. http://dx.doi.org/10.1073/pnas.1323106111

Cheng, Z.J., J. Zhao, Y. Sun, W. Hu, Y.L. Wu, B. Cen, G.X. Wu, and G. Pei. 2000. β-Arrestin differentially regulates the chemokine receptor CXCR4-mediated signaling and receptor internalization, and this implicates multiple interaction sites between β-arrestin and CXCR4. *J. Biol. Chem.* 275:2479–2485. http://dx.doi.org/10.1074/jbc.275.4.2479

Derouet, M., L. Thomas, A. Cross, R.J. Moots, and S.W. Edwards. 2004. Granulocyte macrophage colony-stimulating factor signaling and proteasome inhibition delay neutrophil apoptosis by increasing the stability of Mcl-1. *J. Biol. Chem.* 279:26915–26921. http://dx.doi.org/10.1074/jbc.M313875200

Dessauer, C.W., T.T. Scully, and A.G. Gilman. 1997. Interactions of forskolin and ATP with the cytosolic domains of mammalian adenylyl cyclase. *J. Biol. Chem.* 272:22272–22277. http://dx.doi.org/10.1074/jbc.272.35.22272

Dutt, P., J.F. Wang, and J.E. Groopman. 1998. Stromal cell-derived factor-1α and stem cell factor/*kit* ligand share signaling pathways in hemopoietic progenitors: a potential mechanism for cooperative induction of chemotaxis. *J. Immunol.* 161:3652–3658.

Erdemir, H.H., Z. Li, and D.B. Sacks. 2014. IQGAP1 binds to estrogen receptor-α and modulates its function. *J. Biol. Chem.* 289:9100–9112. http://dx.doi.org/10.1074/jbc.M114.553511

Feigin, M.E., B. Xue, M.C. Hammell, and S.K. Muthuswamy. 2014. G-protein-coupled receptor GPR161 is overexpressed in breast cancer and is a promoter of cell proliferation and invasion. *Proc. Natl. Acad. Sci. USA.* 111:4191–4196. http://dx.doi.org/10.1073/pnas.1320239111

Fernández-Arenas, E., E. Calleja, N. Martínez-Martín, S.I. Gharbi, R. Navajas, N. García-Medel, P. Penela, A. Alcamí, F. Mayor Jr., J.P. Albar, and B. Alarcón. 2014. β-Arrestin-1 mediates the TCR-triggered re-routing of distal receptors to the immunological synapse by a PKC-mediated mechanism. *EMBO J.* 33:559–577. http://dx.doi.org/10.1002/embj.201386022

Finetti, F., S.R. Paccani, M.G. Riparbelli, E. Giacomello, G. Perinetti, G.J. Pazour, J.L. Rosenbaum, and C.T. Baldari. 2009. Intraflagellar transport is required for polarized recycling of the TCR/CD3 complex to the immune synapse. *Nat. Cell Biol.* 11:1332–1339. http://dx.doi.org/10.1038/ncb1977

Finetti, F., L. Patrussi, G. Masi, A. Onnis, D. Galgano, O.M. Lucherini, G.J. Pazour, and C.T. Baldari. 2014. Specific recycling receptors are targeted to the immune synapse by the intraflagellar transport system. *J. Cell Sci.* 127:1924–1937. http://dx.doi.org/10.1242/jcs.139337

Fukata, M., T. Watanabe, J. Noritake, M. Nakagawa, M. Yamaga, S. Kuroda, Y. Matsuura, A. Iwamatsu, F. Perez, and K. Kaibuchi. 2002. Rac1 and Cdc42 capture microtubules through IQGAP1 and CLIP-170. *Cell.* 109:873–885. http://dx.doi.org/10.1016/S0092-8674(02)00800-0

Gendron, L., N. Mittal, H. Beaudry, and W. Walwyn. 2015. Recent advances on the δ opioid receptor: from trafficking to function. *Br. J. Pharmacol.* 172:403–419. http://dx.doi.org/10.1111/bph.12706

Gentilini, A., K. Rombouts, S. Galastri, A. Caligiuri, E. Mingarelli, T. Mello, F. Marra, S. Mantero, M. Roncalli, P. Invernizzi, and M. Pinzani. 2012. Role of the stromal-derived factor-1 (SDF-1)–CXCR4 axis in the interaction between hepatic stellate cells and cholangiocarcinoma. *J. Hepatol.* 57:813–820. http://dx.doi.org/10.1016/j.jhep.2012.06.012

Gomez, T.S., S.D. McCarney, E. Carrizosa, C.M. Labno, E.O. Comiskey, J.C. Nolz, P. Zhu, B.D. Freedman, M.R. Clark, D.J. Rawlings, et al. 2006. HS1 functions as an essential actin-regulatory adaptor protein at the immune synapse. *Immunity.* 24:741–752. http://dx.doi.org/10.1016/j.immuni.2006.03.022

Gorman, J.A., A. Babich, C.J. Dick, R.A. Schoon, A. Koenig, T.S. Gomez, J.K. Burkhardt, and D.D. Billadeau. 2012. The cytoskeletal adaptor protein IQGAP1 regulates TCR-mediated signaling and filamentous actin dynamics. *J. Immunol.* 188:6135–6144. http://dx.doi.org/10.4049/jimmunol.1103487

Goto, T., A. Sato, S. Adachi, S. Iemura, T. Natsume, and H. Shibuya. 2013. IQGAP1 protein regulates nuclear localization of β-catenin via importin-β5 protein in Wnt signaling. *J. Biol. Chem.* 288:36351–36360. http://dx.doi.org/10.1074/jbc.M113.520528

Grundler, R., L. Brault, C. Gasser, A.N. Bullock, T. Dechow, S. Woetzel, V. Pogacic, A. Villa, S. Ehret, G. Berridge, et al. 2009. Dissection of PIM serine/threonine kinases in FLT3-ITD-induced leukemogenesis reveals PIM1 as regulator of CXCL12-CXCR4-mediated homing and migration. *J. Exp. Med.* 206:1957–1970. http://dx.doi.org/10.1084/jem.20082074

Heagy, W., M. Laurance, E. Cohen, and R. Finberg. 1990. Neurohormones regulate T cell function. *J. Exp. Med.* 171:1625–1633. http://dx.doi.org/10.1084/jem.171.5.1625

Hedin, K.E., M.P. Bell, K.R. Kalli, C.J. Huntoon, B.M. Sharp, and D.J. McKean. 1997. δ-Opioid receptors expressed by Jurkat T cells enhance IL-2 secretion by increasing AP-1 complexes and activity of the NF-AT/AP-1-binding promoter element. *J. Immunol.* 159:5431–5440.

Hedin, K.E., M.P. Bell, C.J. Huntoon, L.M. Karnitz, and D.J. McKean. 1999. Gi proteins use a novel beta gamma- and Ras-independent pathway to activate extracellular signal-regulated kinase and mobilize AP-1 transcription factors in Jurkat T lymphocytes. *J. Biol. Chem.* 274:19992–20001. http://dx.doi.org/10.1074/jbc.274.28.19992

Hoeller, D., C.M. Hecker, and I. Dikic. 2006. Ubiquitin and ubiquitin-like proteins in cancer pathogenesis. *Nat. Rev. Cancer.* 6:776–788. http://dx.doi.org/10.1038/nrc1994

Jameson, K.L., P.K. Mazur, A.M. Zehnder, J. Zhang, B. Zarnegar, J. Sage, and P.A. Khavari. 2013. IQGAP1 scaffold-kinase interaction blockade selectively targets RAS-MAP kinase-driven tumors. *Nat. Med.* 19:626–630. http://dx.doi.org/10.1038/nm.3165

Kanwar, N., and J.A. Wilkins. 2011. IQGAP1 involvement in MTOC and granule polarization in NK-cell cytotoxicity. *Eur. J. Immunol.* 41:2763–2773. http://dx.doi.org/10.1002/eji.201040444

Konoplev, S., G.Z. Rassidakis, E. Estey, H. Kantarjian, C.I. Liakou, X. Huang, L. Xiao, M. Andreeff, M. Konopleva, and L.J. Medeiros. 2007. Overexpression of CXCR4 predicts adverse overall and event-free survival in patients with unmutated FLT3 acute myeloid leukemia with normal karyotype. *Cancer.* 109:1152–1156. http://dx.doi.org/10.1002/cncr.22510

Kramer, H.K., M.L. Andria, S.A. Kushner, D.H. Esposito, J.M. Hiller, and E.J. Simon. 2000. Mutation of tyrosine 318 (Y318F) in the delta-opioid receptor attenuates tyrosine phosphorylation, agonist-dependent receptor internalization, and mitogen-activated protein kinase activation. *Brain Res. Mol. Brain Res.* 79:55–66. http://dx.doi.org/10.1016/S0169-328X(00)00097-8

Kremer, K.N., I.C. Clift, A.G. Miamen, A.O. Bamidele, N.X. Qian, T.D. Humphreys, and K.E. Hedin. 2011a. Stromal cell-derived factor-1 signaling via the CXCR4-TCR heterodimer requires phospholipase C-β3 and phospholipase C-γ1 for distinct cellular responses. *J. Immunol.* 187:1440–1447. http://dx.doi.org/10.4049/jimmunol.1100820

Kremer, K.N., A. Kumar, and K.E. Hedin. 2011b. Gαi2 and ZAP-70 mediate RasGRP1 membrane localization and activation of SDF-1–induced T cell functions. *J. Immunol.* 187:3177–3185. http://dx.doi.org/10.4049/jimmunol.1100206

Krishnan, S., G.E. Fernandez, D.B. Sacks, and N.V. Prasadarao. 2012. IQGAP1 mediates the disruption of adherens junctions to promote *Escherichia coli* K1 invasion of brain endothelial cells. *Cell. Microbiol.* 14:1415–1433. http://dx.doi.org/10.1111/j.1462-5822.2012.01805.x

Kumar, A., T.D. Humphreys, K.N. Kremer, P.S. Bramati, L. Bradfield, C.E. Edgar, and K.E. Hedin. 2006. CXCR4 physically associates with the T cell receptor to signal in T cells. *Immunity.* 25:213–224. http://dx.doi.org/10.1016/j.immuni.2006.06.015

Kumar, A., K.N. Kremer, D. Dominguez, M. Tadi, and K.E. Hedin. 2011. Gα13 and Rho mediate endosomal trafficking of CXCR4 into Rab11+ vesicles upon stromal cell-derived factor-1 stimulation. *J. Immunol.* 186:951–958. http://dx.doi.org/10.4049/jimmunol.1002019

Lansbergen, G., Y. Komarova, M. Modesti, C. Wyman, C.C. Hoogenraad, H.V. Goodson, R.P. Lemaitre, D.N. Drechsel, E. van Munster, T.W. Gadella Jr., et al. 2004. Conformational changes in CLIP-170 regulate its binding to microtubules and dynactin localization. *J. Cell Biol.* 166:1003–1014. http://dx.doi.org/10.1083/jcb.200402082

Law, P.Y., O.M. Kouhen, J. Solberg, W. Wang, L.J. Erickson, and H.H. Loh. 2000. Deltorphin II-induced rapid desensitization of δ-opioid receptor requires both phosphorylation and internalization of the receptor. *J. Biol. Chem.* 275:32057–32065. http://dx.doi.org/10.1074/jbc.M002395200

Liu, C., D.D. Billadeau, H. Abdelhakim, E. Leof, K. Kaibuchi, C. Bernabeu, G.S. Bloom, L. Yang, L. Boardman, V.H. Shah, and N. Kang. 2013. IQGAP1 suppresses TβRII-mediated myofibroblastic activation and metastatic growth in liver. *J. Clin. Invest.* 123:1138–1156. http://dx.doi.org/10.1172/JCI63836

Malarkannan, S., A. Awasthi, K. Rajasekaran, P. Kumar, K.M. Schuldt, A. Bartoszek, N. Manoharan, N.K. Goldner, C.M. Umhoefer, and M.S. Thakar. 2012. IQGAP1: a regulator of intracellular spacetime relativity. *J. Immunol.* 188:2057–2063. http://dx.doi.org/10.4049/jimmunol.1102439

Malik, R., and A. Marchese. 2010. Arrestin-2 interacts with the endosomal sorting complex required for transport machinery to modulate endosomal sorting of CXCR4. *Mol. Biol. Cell.* 21:2529–2541. http://dx.doi.org/10.1091/mbc.E10-02-0169

Malik, R., U.J. Soh, J. Trejo, and A. Marchese. 2012. Novel roles for the E3 ubiquitin ligase atrophin-interacting protein 4 and signal transduction adaptor molecule 1 in G protein-coupled receptor signaling. *J. Biol. Chem.* 287:9013–9027. http://dx.doi.org/10.1074/jbc.M111.336792

Marchese, A. 2014. Endocytic trafficking of chemokine receptors. *Curr. Opin. Cell Biol.* 27:72–77. http://dx.doi.org/10.1016/j.ceb.2013.11.011

Marchese, A., and J.L. Benovic. 2001. Agonist-promoted ubiquitination of the G protein-coupled receptor CXCR4 mediates lysosomal sorting. *J. Biol. Chem.* 276:45509–45512. http://dx.doi.org/10.1074/jbc.C100527200

Marchese, A., C. Raiborg, F. Santini, J.H. Keen, H. Stenmark, and J.L. Benovic. 2003. The E3 ubiquitin ligase AIP4 mediates ubiquitination and sorting of the G protein-coupled receptor CXCR4. *Dev. Cell.* 5:709–722. http://dx.doi.org/10.1016/S1534-5807(03)00321-6

Masztalerz, A., I.S. Zeelenberg, Y.M. Wijnands, R. de Bruijn, A.M. Drager, H. Janssen, and E. Roos. 2007. Synaptotagmin 3 deficiency in T cells impairs recycling of the chemokine receptor CXCR4 and thereby inhibits CXCL12 chemokine-induced migration. *J. Cell Sci.* 120:219–228. http://dx.doi.org/10.1242/jcs.03328

Mataraza, J.M., M.W. Briggs, Z. Li, A. Entwistle, A.J. Ridley, and D.B. Sacks. 2003. IQGAP1 promotes cell motility and invasion. *J. Biol. Chem.* 278:41237–41245. http://dx.doi.org/10.1074/jbc.M304838200

Morgan, M.R., H. Hamidi, M.D. Bass, S. Warwood, C. Ballestrem, and M.J. Humphries. 2013. Syndecan-4 phosphorylation is a control point for integrin recycling. *Dev. Cell.* 24:472–485. http://dx.doi.org/10.1016/j.devcel.2013.01.027

Mosesson, Y., G.B. Mills, and Y. Yarden. 2008. Derailed endocytosis: an emerging feature of cancer. *Nat. Rev. Cancer.* 8:835–850. http://dx.doi.org/10.1038/nrc2521

Müller, A., B. Homey, H. Soto, N. Ge, D. Catron, M.E. Buchanan, T. McClanahan, E. Murphy, W. Yuan, S.N. Wagner, et al. 2001. Involvement of chemokine receptors in breast cancer metastasis. *Nature.* 410:50–56. http://dx.doi.org/10.1038/35065016

Nakano, A., H. Kato, T. Watanabe, K.D. Min, S. Yamazaki, Y. Asano, O. Seguchi, S. Higo, Y. Shintani, H. Asanuma, et al. 2010. AMPK controls the speed of microtubule polymerization and directional cell migration through CLIP-170 phosphorylation. *Nat. Cell Biol.* 12:583–590. http://dx.doi.org/10.1038/ncb2060

Neel, N.F., E. Schutyser, J. Sai, G.H. Fan, and A. Richmond. 2005. Chemokine receptor internalization and intracellular trafficking. *Cytokine Growth Factor Rev.* 16:637–658. http://dx.doi.org/10.1016/j.cytogfr.2005.05.008

Neel, N.F., J. Sai, A.J.L. Ham, T. Sobolik-Delmaire, R.L. Mernaugh, and A. Richmond. 2011. IQGAP1 is a novel CXCR2-interacting protein and essential component of the "chemosynapse". *PLoS ONE.* 6:e23813. http://dx.doi.org/10.1371/journal.pone.0023813

Nieto, M., J.M. Frade, D. Sancho, M. Mellado, C. Martinez-A, and F. Sánchez-Madrid. 1997. Polarization of chemokine receptors to the leading edge during lymphocyte chemotaxis. *J. Exp. Med.* 186:153–158. http://dx.doi.org/10.1084/jem.186.1.153

Pierre, P., J. Scheel, J.E. Rickard, and T.E. Kreis. 1992. CLIP-170 links endocytic vesicles to microtubules. *Cell.* 70:887–900. http://dx.doi.org/10.1016/0092-8674(92)90240-D

Provance, D.W. Jr., C.R. Gourley, C.M. Silan, L.C. Cameron, K.M. Shokat, J.R. Goldenring, K. Shah, P.G. Gillespie, and J.A. Mercer. 2004. Chemical-genetic inhibition of a sensitized mutant myosin Vb demonstrates a role in peripheral-pericentriolar membrane traffic. *Proc. Natl. Acad. Sci. USA.* 101:1868–1873. http://dx.doi.org/10.1073/pnas.0305895101

Rizvi, S., and G.J. Gores. 2013. Pathogenesis, diagnosis, and management of cholangiocarcinoma. *Gastroenterology.* 145:1215–1229. http://dx.doi.org/10.1053/j.gastro.2013.10.013

Roy, M., Z. Li, and D.B. Sacks. 2005. IQGAP1 is a scaffold for mitogen-activated protein kinase signaling. *Mol. Cell. Biol.* 25:7940–7952. http://dx.doi.org/10.1128/MCB.25.18.7940-7952.2005

Sharp, B.M., N.A. Shahabi, W. Heagy, K. McAllen, M. Bell, C. Huntoon, and D.J. McKean. 1996. Dual signal transduction through delta opioid receptors in a transfected human T-cell line. *Proc. Natl. Acad. Sci. USA.* 93:8294–8299. http://dx.doi.org/10.1073/pnas.93.16.8294

Shen, W., L.J. Bendall, D.J. Gottlieb, and K.F. Bradstock. 2001. The chemokine receptor CXCR4 enhances integrin-mediated in vitro adhesion and facilitates engraftment of leukemic precursor-B cells in the bone marrow. *Exp. Hematol.* 29:1439–1447. http://dx.doi.org/10.1016/S0301-472X(01)00741-X

Shenoy, S.K., and R.J. Lefkowitz. 2005. Receptor-specific ubiquitination of β-arrestin directs assembly and targeting of seven-transmembrane receptor signalosomes. *J. Biol. Chem.* 280:15315–15324. http://dx.doi.org/10.1074/jbc.M412418200

Stuart, D.D., and W.R. Sellers. 2013. Targeting RAF-MEK-ERK kinase-scaffold interactions in cancer. *Nat. Med.* 19:538–540. http://dx.doi.org/10.1038/nm.3195

Teicher, B.A., and S.P. Fricker. 2010. CXCL12 (SDF-1)/CXCR4 pathway in cancer. *Clin. Cancer Res.* 16:2927–2931. http://dx.doi.org/10.1158/1078-0432.CCR-09-2329

Tsao, P.I., and M. von Zastrow. 2000. Type-specific sorting of G protein-coupled receptors after endocytosis. *J. Biol. Chem.* 275:11130–11140. http://dx.doi.org/10.1074/jbc.275.15.11130

White, C.D., M.D. Brown, and D.B. Sacks. 2009. IQGAPs in cancer: a family of scaffold proteins underlying tumorigenesis. *FEBS Lett.* 583:1817–1824. http://dx.doi.org/10.1016/j.febslet.2009.05.007

White, C.D., Z. Li, D.A. Dillon, and D.B. Sacks. 2011. IQGAP1 protein binds human epidermal growth factor receptor 2 (HER2) and modulates trastuzumab resistance. *J. Biol. Chem.* 286:29734–29747. http://dx.doi.org/10.1074/jbc.M111.220939

White, C.D., H.H. Erdemir, and D.B. Sacks. 2012. IQGAP1 and its binding proteins control diverse biological functions. *Cell. Signal.* 24:826–834. http://dx.doi.org/10.1016/j.cellsig.2011.12.005

Zeng, Z., Y.X. Shi, I.J. Samudio, R.Y. Wang, X. Ling, O. Frolova, M. Levis, J.B. Rubin, R.R. Negrin, E.H. Estey, et al. 2009. Targeting the leukemia microenvironment by CXCR4 inhibition overcomes resistance to kinase inhibitors and chemotherapy in AML. *Blood.* 113:6215–6224. http://dx.doi.org/10.1182/blood-2008-05-158311

Zhang, X., F. Wang, X. Chen, J. Li, B. Xiang, Y.Q. Zhang, B.M. Li, and L. Ma. 2005. β-Arrestin1 and β-arrestin2 are differentially required for phosphorylation-dependent and -independent internalization of δ-opioid receptors. *J. Neurochem.* 95:169–178. http://dx.doi.org/10.1111/j.1471-4159.2005.03352.x

Zugaza, J.L., M.J. Caloca, and X.R. Bustelo. 2004. Inverted signaling hierarchy between RAS and RAC in T-lymphocytes. *Oncogene.* 23:5823–5833. http://dx.doi.org/10.1038/sj.onc.1207768